SARS-CoV-2 antigen exposure history shapes phenotypes and specificity of memory CD8 T cells

Anastasia A. Minervina[1#], Mikhail V. Pogorelyy[1#], Allison M. Kirk[1], Jeremy Chase Crawford[1], E. Kaitlynn Allen[1], Ching-Heng Chou[1], Robert C. Mettelman[1], Kim J. Allison[2], Chun-Yang Lin[1], David C. Brice[1], Xun Zhu[3], Kasi Vegesana[4], Gang Wu[3], Sanchit Trivedi[5], Pratibha Kottapalli[5], Daniel Darnell[5], Suzanne McNeely[5], Scott R. Olsen[5], Stacey Schultz-Cherry[2], Jeremie H. Estepp[6], the SJTRC Study Team✤, Maureen A. McGargill[1], Joshua Wolf[2], Paul G. Thomas[1]

[1] Department of Immunology, St. Jude Children's Research Hospital, Memphis, TN USA
[2] Department of Infectious Diseases, St. Jude Children's Research Hospital, Memphis, TN USA
[3] Center for Applied Bioinformatics, St. Jude Children's Research Hospital, Memphis, TN USA
[4] Information Services, St. Jude Children's Research Hospital, Memphis, TN USA
[5] Hartwell Center for Bioinformatics & Biotechnology, St. Jude Children's Research Hospital, Memphis, TN USA
[6] Department of Global Pediatric Medicine, St. Jude Children's Research Hospital, Memphis, TN USA

#Equal contribution

✤ Aditya Gaur, James Hoffman, Motomi Mori, Li Tang, Elaine Tuomanen, Richard Webby, Hana Hakim, Randall T. Hayden, Diego R. Hijano, Resha Bajracharya, Walid Awad, Lee-Ann Van de Velde, Brandi L. Clark, Taylor L. Wilson, Aisha Souquette, Ashley Castellaw, Ronald H. Dallas, Jason Hodges, Ashleigh Gowen, Jamie Russell-Bell, James Sparks, David E. Wittman, Thomas P. Fabrizio, Sean Cherry, Ericka Kirkpatrick Roubidoux, Valerie Cortez, Pamela Freiden, Nicholas Wohlgemuth, Kendall Whitt;

Correspondence to Joshua Wolf joshua.wolf@stjude.org and Paul Thomas paul.thomas@stjude.org

Abstract

Although mRNA vaccine efficacy against severe COVID-19 remains high, variant emergence and breakthrough infections have changed vaccine policy to include booster immunizations. However, the effect of diverse and repeated antigen exposures on SARS-CoV-2 memory T cells is poorly understood. Here, we utilize DNA-barcoded MHC-multimers combined with scRNAseq and scTCRseq to capture the *ex vivo* profile of SARS-CoV-2-responsive T cells within a cohort of individuals with one, two, or three antigen exposures, including vaccination, primary infection, and breakthrough infection. We found that the order of exposure determined the relative distribution between spike- and non-spike-specific responses, with vaccination after infection leading to further expansion of spike-specific T cells and differentiation to a CCR7-CD45RA+ effector phenotype. In contrast, individuals experiencing a breakthrough infection mount vigorous non-spike-specific responses. In-depth analysis of over 4,000 epitope-specific T cell receptor sequences demonstrates that all types of exposures elicit diverse repertoires characterized by shared, dominant TCR motifs, with no evidence for repertoire narrowing from repeated exposure. Our findings suggest that breakthrough infections diversify the T cell memory repertoire and that current vaccination protocols continue to expand and differentiate spike-specific memory responses.

The continued evolution of SARS-CoV-2 into diverse lineages has led to reduced efficacy of neutralizing antibody responses raised against ancestral strains, including those used in all approved vaccine formulations. Individuals receiving two doses of mRNA vaccine BNT162b2 experienced a dramatic loss in neutralization titers against the Omicron variant[1]. While current protection studies have focused on antibody responses as the key effector mechanism that limits infection, CD8 T cells are likely to play critical roles in the prevention of severe disease[2–6]. Indeed, there are case reports of patients with impaired humoral immunity where efficient T cell responses appear sufficient for viral clearance[7,8].

In response to the changing landscape of viral evolution and spread, vaccine recommendations have been continually updated to include a booster dose, representing a third immunization at least six months after the initial dose of the Pfizer/BioNTech or Moderna mRNA vaccines. Despite these measures, significant numbers of so-called "breakthrough" COVID-19 cases are being recorded, with individuals becoming infected after two or three vaccine doses or even after prior infection. In all of these settings, adaptive immunity is repeatedly exposed to SARS-CoV-2 antigens, and the effects of this recurrent boosting on the functional profile, magnitude, and specificity distribution of responding T cells remain poorly understood[9,10]. In particular, it is largely unknown if repeated exposure to the same SARS-CoV-2 antigens boosts pre-existing T cell memory and, further, if an exposure to a novel antigen (e.g, infection after vaccination or infection with a new viral variant) induces *de novo* memory and diversifies the TCR repertoire, or instead preferentially expands previously primed responses.

CD8 T cells recognize antigen presented on the cell surface by the Class I Major Histocompatibility Complex (MHC), which is encoded by the most polymorphic genes in the human population (Human Leukocyte Antigen, HLA genes)[11]. Variability of peptide-MHC across and within donors makes measuring epitope-specific T cell responses challenging, and as a result, studies often rely on bulk response assays (e.g., peptide stimulation). Although peptide stimulation assays in principle can provide an estimate of the total magnitude of the CD8 response, they underestimate the frequency of epitope-specific T cells[12] Further, because these assays require cellular activation to detect a response, they prevent the direct assessment of cell phenotypes *ex vivo*. Staining with MHC-multimers loaded with individual peptides is an alternative approach,

81 which requires pre-selection of immunogenic peptides. Several SARS-CoV-2 epitopes presented
82 by common HLA alleles were discovered in the past two years, permitting the tracking of epitope-
83 specific T cell responses in infected[13–26] and vaccinated individuals[9,12] using MHC-multimers.
84
85 Here we utilized DNA-barcoded MHC-dextramers with subsequent scRNAseq and scTCRseq to
86 investigate the effects of repeated antigen exposures (SARS-CoV-2 infections and vaccinations
87 with Pfizer/Biontech BNT162b2) on the key features of the CD8 T cell response, including
88 response magnitude, functional gene expression profiles (assessed directly *ex vivo*), and the
89 constituent T cell receptor repertoire. In other contexts, persistent exposure to antigen has been
90 shown to drive various forms of T cell dysfunction, including exhaustion[27]. Further, the focused
91 priming on SARS-CoV-2 spike antigens, the only component of all approved vaccines, may bias
92 subsequent responses during a breakthrough infection towards recall to spike. Thus, it is crucial to
93 understand how pre-existing T cell memory impacts the immune response and memory formation
94 to novel SARS-CoV-2 antigens after repeated exposures.
95
96 **Results**
97 *Antibody responses to SARS-CoV-2 infection and vaccination*
98 To investigate the effect of repeated SARS-CoV-2 antigen exposure on pre-existing memory T
99 cells, we selected a cohort of 55 individuals from SJTRC, a prospective, longitudinal study of St.
100 Jude Children's Research Hospital adult (≥18 years old) employees (Fig. 1a). Sixteen of these
101 participants remained negative for SARS-CoV-2 during weekly PCR testing (naive, N1-N16),
102 whereas 30 of the subjects were diagnosed as SARS-CoV-2 positive with a PCR test and recovered
103 from mild disease (recovered, R1-R30) during the study period. Both the naive and recovered
104 groups received two doses of the Pfizer-BioNTech BNT162b2 mRNA vaccine, and plasma and
105 PBMC samples were collected for all subjects after the second dose of vaccine and at various
106 earlier time points. This produced four subgroups with distinct antigen exposure combinations:
107 infection only (inf, R1-R16), vaccinated only (vax2, N1-N16), infected followed by one dose of
108 vaccine (inf-vax1, R17-R26), and infected followed by two doses of vaccine (inf-vax2, R1-R26).
109 All inf and inf-vax1 subjects were also sampled after their second dose of vaccine, and therefore
110 have matched samples in the inf-vax2 group (Fig. 1b). Additionally, we collected samples from 9
111 donors who tested positive for SARS-CoV-2 after receiving both doses of BNT162b2 and

experienced symptomatic breakthrough infection (vax2-inf, or "breakthrough" group, B1-B9). As expected, the only group negative for N-protein specific antibodies was the vax2 group that was not infected with SARS-CoV-2 (Extended data Fig. 1a). In concordance with previous reports[28–30], we observed anti-RBD (Fig. 1c, Extended data Fig. 1b) and anti-spike protein IgG (Extended data Fig. 1c) boost after vaccination of recovered individuals. Also in line with other studies[28–33], most of the antibody boost in SARS-CoV-2 recovered individuals is caused by the first rather than the second vaccine dose, as only two donors (R20, R26) showed a boost in anti-RBD antibody levels after the second vaccine dose, while antibody levels in other donors remained stable (Extended data Fig. 1b). Overall, anti-RBD (Fig. 1c) and anti-spike IgG levels (Extended data Fig. 1c) were similar between vax2 and inf-vax groups. However, breakthrough cases exhibited significantly, but not dramatically, lower anti-RBD and anti-spike antibody levels after infection compared to both vax2 and inf-vax2 individuals (Fig. 1c).

Magnitude of epitope-specific CD8$^+$ T cell response to mRNA infection and vaccination

To evaluate epitope-specific CD8$^+$ T cell responses to SARS-CoV-2 antigen exposure, we investigated previously published data for spike-derived epitopes with a resolved HLA-restriction confirmed in multiple publications. This search resulted in the selection of six spike protein epitopes presented on the HLA alleles A*01:01, A*02:01, A*24:02, B*15:01, and B*44:02[13,15,17,20,24–26,34–36]. We then added 12 previously described non-spike epitopes presented on the same HLA molecules, resulting in a total panel of 18 SARS-CoV-2 epitopes (Fig. 1d, Extended data Table 1). In addition, four of the selected epitopes (A24_VYI, B15_NQK, B44_AEV and B44_VEN) were highly similar to orthologs from common cold coronaviruses (CCCoV), and the CCCoV variant pMHC-dextramers were also included to test the cross-reactive potential of these epitopes[37–40].

PBMCs from each donor were stained with a panel of DNA-barcoded, fluorescently labeled dextramers (Fig. 1a, Extended data Table 1) that matched the donor's HLA alleles (Extended data Table 2). For vax2 donors, these panels only included spike-derived dextramers. Epitope-specific T cells (CD3$^+$CD8$^+$dextramer$^+$ cells) were isolated using FACS (Extended data Fig. 2) and then assayed with scRNAseq, scTCRseq, and CITEseq using the 10x Chromium platform. We observed a detectable (>0.01%) dextramer-positive CD8$^+$ T cell response in 15/16 vaccinated donors that

143 were not previously infected and in 37/39 SARS-CoV-2-infected donors. Although the overall
144 frequency of dextramer-specific cells was low (0.41±0.17% SEM of $CD8^+$ T cells; range: 0.01-
145 14.1% of $CD8^+$ T cells), it was comparable to the epitope-specific memory cell frequencies
146 observed months after challenge in other studies of SARS-CoV-2 infection[13,17,20,21], even though
147 these studies frequently used peptide stimulation covering an entire protein or multiple proteins.
148 Furthermore, the absolute magnitude of the epitope-specific T cell responses was similar across
149 all groups (Fig. 1e) despite varying sources (vaccine/infection) of antigen exposure ($p>0.05$ for all
150 pairwise comparisons, Mann-Whitney U test with Benjamini-Hochberg multiple testing
151 correction).
152
153 *HLA-B*15:01 presents a spike-derived epitope cross-reactive to CCCoV*
154 Use of the DNA-barcoded dextramers allowed us to deconvolve the overall T cell response to 18
155 distinct epitope-specific responses. For each cell, we calculated the number of unique molecular
156 identifiers (UMIs) per dextramer, and considered a cell as dextramer-specific if more than 30% of
157 the dextramer-derived UMIs corresponded to that dextramer's specific barcode. Cells that did not
158 match the criteria (i.e., exhibited ambiguous binding or fewer than 4 UMIs per most abundant
159 dextramer) were considered unspecific binders and were excluded from the dataset. This resulted
160 in non-overlapping dextramer-positive and -negative groups of cells for each dextramer (Fig. 2a,
161 Extended data Fig. 3). To further assess this threshold, we considered the dextramer assignment
162 of individual cells among the 43 most abundant T cell clones (i.e., clonotypes with ≥ 20 cells) as
163 defined by scTCRseq. Of these clonotypes, 72% (31/43) matched a single epitope across all cells
164 (Fig. 2b), with only six of the most abundant clonotypes assigned to several non-orthologous
165 epitopes. However, for all these clonotypes, there was a clear dominant epitope assigned to the
166 majority of cells, demonstrating the general robustness of the dextramer specificity thresholds.
167 Interestingly, five of the most abundant TCR clonotypes were assigned to both B15-NQK_Q
168 SARS-CoV-2 and B15-NQK_A CCCoV (HKU1/OC43) orthologs of the spike epitope, supporting
169 our initial hypothesis for potential SARS-CoV-2/CCCoV epitope cross-reactivity. Indeed, the
170 UMI counts for the dextramers with SARS-CoV-2 and CCCoV variants of the epitope were
171 strongly correlated (Fig. 2c), suggesting that the exact same cells can bind both versions of the
172 epitope.
173

174 To further validate that a single TCR could recognize both variants of B15-NQK, we made a Jurkat
175 cell line expressing one of the potentially cross-reactive αβTCRs. This T cell line recognized both
176 CCCoV and SARS-CoV-2 variants of the peptide, as demonstrated by HLA-B*15:01-multimer
177 staining (Fig. 2d) and peptide stimulation assays (Extended data Fig. 4). Interestingly, the presence
178 of T cells specific to this epitope coincided with higher IgG levels against the spike protein of
179 common cold betacoronaviruses HKU1 and OC43 prior to infection or vaccination (Extended data
180 Fig. 5). These data indicate that SARS-CoV-2 may reactivate cross-reactive memory $CD8^+$ T cells
181 established during previous OC43/HKU1 infections.
182
183 *Spike vs. non-spike response distribution varies with antigen exposures*
184 Because barcoded dextramers allow us to simultaneously measure the response to multiple
185 epitopes in the same sample at single-cell resolution, we also utilized these data to compare the
186 magnitude of the response to different epitopes. Among all the tested epitopes, A01_TTD,
187 A01_LTD, A02_YLQ, and B15_NQK elicited the strongest overall response (Fig. 2e) and were
188 also found in the majority of HLA-matched samples. Although we observed responses to all other
189 epitopes, they occurred at lower frequencies and only in a subset of HLA-matched donors.
190
191 Donors with distinct HLA alleles present different subsets of epitopes. Thus, to robustly compare
192 the magnitude of spike and non-spike responses, we characterized the contribution of each of the
193 six A*01:01 restricted epitopes in HLA-A*01:01-positive SARS-CoV-2 convalescent individuals
194 (n=13). Interestingly, the proportion of the spike-derived epitope A01_LTD response significantly
195 increased in inf-vax2 individuals compared to infected individuals prior to vaccination (0.8%
196 A01_LTD-specific cells of total A01-restricted response for inf-only group, vs 48% A01_LTD-
197 specific cells of total A01-restricted response for inf-vax2, $p<0.0001$ Fisher exact test; Fig. 2f).
198 Similar but less striking effects were also observed within HLA-A*02:01-positive individuals
199 (n=19) for three A*02:01 restricted epitopes (33% of A02_YLQ-specific cells for inf-only, vs 82%
200 of A02_YLQ-specific cells for inf-vax2, $p<0.0001$ Fisher exact test; Extended data Fig. 6). These
201 patterns suggest that the distribution of T cell specificities was shifted towards spike-derived
202 epitopes following vaccination of these previously infected donors (Fig. 2g, Extended data Fig. 7).
203 Indeed, among all donors regardless of HLA type, we observed a significant increase in the fraction
204 of the spike-specific T cell response after vaccination, indicating the recall of epitope-specific

205 memory T cells among previously infected individuals as a result of vaccination (Fig. 2H, p=0.025,
206 one-sided Wilcoxon signed-rank test). Similar to the antibody response, most of this expansion
207 was likely due to the first rather than second dose of the vaccine, as we did not observe a T cell
208 boost between the first and second doses of vaccine in 7/10 subjects (Extended data Fig. 8). In
209 sum, vaccination is able to potently and selectively expand spike-specific responses.
210
211 Given the potent induction and expansion of spike-specific responses by vaccination, even in
212 individuals who were previously infected, we predicted that infection of previously vaccinated
213 individuals (breakthrough, vax2-inf) would maintain a spike-specific bias. Surprisingly, we
214 observed a large non-spike-specific T cell response in the majority of the breakthrough 6/7 (vax2-
215 inf) cohort (Fig. 2h), indicating that a robust primary response to non-spike SARS-CoV-2 antigens
216 during the breakthrough infection is not impaired by the presence of spike-specific immune
217 memory elicited by vaccination. The ratio between spike- and non-spike-specific T cells in
218 breakthrough cases (vax2-inf) was no different from that of donors who were only infected (inf;
219 p=0.97, Mann-Whitney U test), indicating that the T cell response to the non-spike antigens is of
220 comparable magnitude among those who were only infected and and those who experienced
221 breakthrough infection after vaccination (vax2-inf). Thus, while the magnitude of the epitope-
222 specific responses is similar across all exposure types, the composition of epitope-specific
223 responses is clearly skewed by both the number and order of exposures.
224
225 *Phenotypes of epitope-specific CD8$^+$ T cells following SARS-CoV-2 infection and vaccination*
226 To understand if different types of antigen exposures could also drive divergent phenotypes among
227 epitope-specific T cells, we leveraged the single-cell gene expression (scGEX) data corresponding
228 to our TCR and dextramer data. Unsupervised clustering identified 11 distinct transcriptional
229 subsets of epitope-specific cells (Fig. 3a). These clusters were manually annotated using the
230 surface abundance of conventional memory markers (CCR7 and CD45RA) measured by CITEseq
231 (Fig. 3b) and other well-studied expression markers (Fig 3c, Extended data Table 3, Table 4),
232 allowing us to identify the following populations: Transitional Memory (Effector
233 memory(EM)/EM with re-expression of CD45RA(EMRA)), EMRA-like, Central Memory
234 (CM)/T stem cell-like memory (Tscm), Differentiated effectors, naive/Tscm, EM, Resting
235 effectors, EM with exhaustion markers, Resting memory, CM with *GATA3*, and Cycling. Though

236 the proportions of these T cell populations varied substantially across antigen exposure contexts,
237 each gene expression cluster contained cells from all five exposure groups (Fig. 3d, Extended data
238 Fig. 9, 10, 11). Natural infection, breakthrough cases, and vaccination led to the formation of
239 potent T cell memory, including highly cytotoxic populations (clusters 0,1,3,5) and populations
240 with expression of common markers of durable cellular memory (clusters 2,4,8,9), e.g. *TCF7,*
241 *IL7R,* and *CCR7* (Fig. 3c).
242
243 *Repeated exposures cause a shift of T cell memory phenotypes towards EMRA*
244 To determine if a vaccine-induced recall response affects the phenotypes of T cells, we compared
245 the GEX cluster distribution between inf-only and inf-vax2 donors. We observed a significant
246 post-vaccination shift towards a more highly differentiated effector phenotype (EMRA, cluster 1)
247 of spike-specific cells (Fig. 3e, S10, $p<0.0001$, Fisher exact test). Interestingly, there was no such
248 change for non-spike-specific cells, suggesting that vaccination specifically increased the
249 proportion of cells in cluster 1 (EMRA-like) among SARS-CoV-2 recovered donors via a recall of
250 spike-specific memory T cells (Fig. 3f). Indeed, inf-vax1 and inf-vax2 groups were characterized
251 by spike-specific T cells with higher *GZMB, GZMH, GNLY,* and *NKG7* expression and lower
252 *TCF7, IL7R, SELL,* and *LTB* expression than those in other groups, consistent with the EMRA
253 phenotype (Fig. 3g). Interestingly, the spike-specific T cells in breakthrough infections (vax2-inf)
254 exhibited expression profiles more similar to groups with a single type of antigen exposure (vax2
255 or inf) than to those of inf-vax1,2 subjects.
256
257 *Repeated SARS-CoV-2 antigen exposure does not lead to an exhausted T cell phenotype*
258 Repeated or chronic antigen exposure leads to T cell exhaustion in multiple experimental models[27].
259 Several publications have linked T cell exhaustion to an impaired SARS-CoV-2 cellular
260 response[41–43]. While our epitope-specific data similarly included a cluster with high expression of
261 classical exhaustion markers (cluster 7, EM-Ex, Fig. 3c), including *CTLA-4, PD-1, TOX,* and
262 *TIGIT*, this cluster was present in multiple donors (26/51) across all groups, including vax2-only
263 (Extended data Fig. S9, S10). In concordance with previous reports[23,42], this "exhausted cluster"
264 was extremely clonal in composition (Extended data Fig. 12), with more than 70% of the cluster
265 repertoire occupied by just 10 clones (Fig. 3h). We also observed that the number of cells in the
266 "exhausted cluster" within a patient strongly correlated with the number of cells in the cluster of

267 cycling cells (Fig. 3i). Thus, the presence of the exhausted cluster is connected to both clonal
268 expansion and cell proliferation, suggesting that donors who have such cells are still in the active
269 rather than memory state of the CD8 T cell response. To test this, we looked at the distribution of
270 cells among clusters at two available time points after infection (Fig. 1b, donors R1-R30, average
271 time between timepoints was 75.5 days, range 40-126). The number of cells in cluster 7 declined
272 with time (Extended data Fig. 13), indicating that this "exhausted" subset is both common among
273 mild infections yet transient and, importantly, that the presence of these cells is not sufficient to
274 cause notable pathology. Rather, the exhaustion phenotype appears primarily correlated with time
275 since antigen exposure.
276
277 *Convergent and diverse TCR repertoire of epitope-specific CD8$^+$ cells*
278 Our data thus far indicate that vaccination after infection boosts pre-existing T cell memory to
279 spike antigens and leads to significant alterations in the cellular phenotypes. We next asked
280 whether this recall response affects the diversity of the underlying recruited T cell receptor
281 repertoires, potentially narrowing repertoire diversity after each exposure. To compare the TCR
282 repertoires of epitope-specific cells elicited in response to different exposure contexts, we assessed
283 the overall TCRβ repertoire diversity (represented by normalised Shannon entropy). The diversity
284 of both spike- (Fig. 3j) and non-spike-specific repertoires (Fig. 3k) was comparable among all
285 groups (p=0.63 for spike, p=0.17 for non-spike, Kruskal-Wallis H test), suggesting that a diverse
286 repertoire of T cells persists in the memory compartment regardless of antigenic history and is not
287 narrowed by the recall response. This is especially notable among the breakthrough infections, as
288 it indicates that these individuals mount *de novo* diverse non-spike-specific T cell memory in
289 response to the infection.
290
291 We and others have previously shown that T cells recognizing the same epitopes frequently have
292 highly similar T cell receptor sequences[44–46]. We therefore constructed a similarity network of
293 paired, unique αβTCR sequences from our data (Extended data, Table 5), using a threshold on the
294 TCRdist[44] similarity measure to identify highly similar clonotypes (Fig. 4a). The clusters of similar
295 sequences almost exclusively consisted of TCRs with the same epitope specificity and feature
296 biases in V-segment usage (Extended data Fig. 14, 15, 16), as well as striking positional
297 enrichment of certain amino acid residues within the CDR3 region (Fig. 4b). We next individually

298 cloned 12 of these TCRs from the 7 largest similarity clusters into a TCR-null Jurkat cell line
299 (Extended data, Table 6). The resulting cell lines exhibited the expected specificity based on
300 dextramer barcodes both in peptide stimulation assays (Extended data Fig. 17) and dextramer
301 staining (Extended data Fig. 18), validating both the bioinformatics approach and the reagents. We
302 next asked if the same motifs were recruited into the response across antigen exposure histories.
303 Importantly, many of the confirmed CDR3 motifs from spike-specific TCRs were shared among
304 donors who recovered from natural infection, including breakthrough infections, and among
305 immunologically naive donors after vaccination (Fig. 4c). This suggests that epitope recognition
306 is achieved by the same TCR-pMHC molecular interactions regardless of the method of antigen
307 exposure, and thus one could expect similar specificity to potential epitope variants for memory T
308 cells elicited by vaccination or natural infection.
309
310 *TCR motifs recognize most mutated epitopes in SARS-CoV-2 variants*
311 Our TCR analyses established that regardless of antigen history, the same dominant TCR motifs
312 were utilized by subjects responding to a number of important SARS-CoV-2 epitopes. Thus, these
313 TCRs can be used to probe how memory responses from these exposures will detect epitopes in
314 variant SARS-CoV-2 strains. To investigate the potential impact of SARS-CoV-2 variants on T
315 cell recognition, we searched the GISAID for mutations in the selected CD8 epitopes. Mutations
316 in both current and previous viral lineages were included in the analysis if they appeared in at least
317 10% of a Pango lineage and in at least ten thousand isolates. Notably, no mutations in the studied
318 epitopes were observed in the Omicron variant. However, we identified 10 mutations among the
319 200 Pango lineages, including Delta and Gamma WHO variants of concern. Models predicting
320 peptide-MHC binding (NetMHCpan4.1b[47]) suggest that these mutations do not impact the binding
321 of the epitope to the restricting HLA allele, as both mutated and wild-type epitope variants are
322 predicted to be strong binders (Extended data Table 7). Thus, we decided to test whether our
323 transgenic TCR lines were capable of recognizing these mutated epitopes. All three mutated
324 epitopes of A01_TTD could be recognized by at least one of our A01_TTD-specific T cell lines.
325 (Extended data, Fig. 19). Interestingly, one of the mutated A01_TTD epitopes (TT*N*PSFLGRY)
326 was recognized by one of the two generated TCR lines, highlighting the importance of TCR
327 diversity in the cross-reactivity to novel variants. Neither A02_YLQ-specific TCR line was
328 activated by the mutant S:P272L epitope YLQPRTFLL (Extended data, Fig. 19), confirming the

329 data from Dolton et al. This mutation was speculated to play a role in a second Europe COVID-19
330 wave in summer-autumn of 2020[48]. However, none of the currently abundant SARS-CoV-2
331 variants bear this or any other variant of the A02_YLQ epitope at large frequency. Of the four
332 mutations observed in the A24_NYN epitope, two escaped recognition by both cloned TCR lines
333 (Extended data, Fig. 19). The mutation L452R affecting A24_NYN is of particular interest as it is
334 present in over 95% of all Delta variant sequences in GISAID. Whether individuals infected by
335 the Delta variant could utilize other TCR motifs to recognise this mutated epitope requires further
336 investigation. Together, our data suggest that the T cell memory repertoire established by SARS-
337 CoV-2 infection or vaccination has great cross-reactivity potential against novel viral variants, and
338 further shows that not all of the viral mutations affecting T cell epitopes result in the T cell immune
339 escape, even from the most public TCR clones.
340
341 **Discussion**
342
343 Understanding the effects of multiple antigen exposures, in various contexts, on the development
344 of effective $CD8^+$ T cell memory against SARS-CoV-2 is important for determining susceptibility
345 to subsequent infections and the potential for booster vaccination to improve outcomes. To address
346 this, we analyzed multiple parameters of the $CD8^+$ T cell response across five types of antigen
347 exposure history and found that repeated antigen exposures (up to three) continued to induce
348 expansion to the included antigens and drive further functional maturation. Despite this, the
349 underlying TCR repertoire structure within epitope specific responses maintained diversity, which
350 is a promising indication of continued vaccine efficacy. Narrowing of TCR diversity has been
351 shown in a number of contexts to correlate with poor immunological control. As fourth boosters
352 and increased rates of breakthrough infections are providing additional exposures, these data are a
353 useful benchmark for determining how these relatively rapid repeat exposures will continue to
354 mature the response. Close monitoring of these important parameters—magnitude, functional
355 profile, and repertoire diversity—should be continued in longitudinal cohorts with diverse antigen
356 exposures.
357
358 Breakthrough infections of vaccinated individuals have a much lower risk of causing severe
359 disease but are a concern for maintaining transmission and exposing vulnerable populations.

360 Furthermore, breakthrough infections have increased with greater serological drift in emerging
361 variants of concern, including Delta and Omicron. We found that functional profiles among
362 breakthrough infections (vax2-inf) were distinct from other forms of antigen exposure but
363 consistent with effector T cell differentiation and, in fact, demonstrated an arguably earlier
364 differentiation state than inf-vax2 individuals. In addition, we show that these individuals form
365 non-spike specific T cell memory at robust levels, indicating that there is not an intrinsic defect
366 among these individuals in mounting robust anti-SARS-CoV-2 responses and diversifying the T
367 cell memory pool to SARS-CoV-2 internal proteins. The proportion of breakthrough subject
368 response targeting spike epitopes was in fact smaller than that of the inf-vax2 subjects, indicating
369 that individuals with breakthrough infection were not preferentially biased towards spike
370 responses. This is especially important given the continued emergence of SARS-CoV-2
371 variants[10,49–51] and the current uprise in breakthrough infection rate.
372
373 In the midst of characterizing T cell responses against SARS-CoV-2-specific epitopes, we also
374 discovered T cells that are cross-reactive for SARS-CoV-2 and common cold coronavirus variants
375 of an HLA-B*15-restricted immunodominant epitope. The possibility of this cross-reactivity was
376 hypothesized previously[52], where the clonotypes with this TCR motif were the most expanded in
377 an HLA-B*15 positive donor. An epitope from N-protein HLA-B*07_SPR has also been shown
378 to be cross-reactive with HKU1 and OC43 common cold coronaviruses[14,53], although other studies
379 of T cells specific to these epitopes concluded they were not cross-reactive[5,18]. The extent of
380 protection in HLA-B*15+ and HLA-B*07+ donors recently infected with common cold
381 coronaviruses is yet to be determined, but a high frequency of cross-reactive CD8 T cells may
382 correlate with protection.
383
384 The most striking differences we observed based on antigenic history were in the phenotype of
385 elicited cells. In particular, we found an increase in the fraction of EMRA spike-specific T cells
386 following vaccination in previously infected subjects (inf-vax2). It remains unclear whether the
387 EMRA phenotype is associated with more or less durable and efficient protection, and longer
388 follow-up studies of the durability of memory in vax2-only, inf-only, and inf-vax2 groups should
389 closely monitor the phenotype of antigen-specific T cell responses and their persistence. This is

390 particularly relevant given the current routine practice of third, and soon possibly fourth, vaccine
391 doses.
392
393 Precise measurement of epitope-specific T cell and B cell responses is crucial for defining the
394 correlates of SARS-CoV-2 protection, which will inform vaccination strategies to prevent
395 pandemic recurrence as additional SARS-CoV-2 variants emerge. The striking similarity between
396 the magnitude and constituent repertoires of epitope-specific CD8 T cell responses following
397 infection, vaccination, or infection followed by vaccination, indicate that mRNA vaccines are
398 capable of inducing nearly equivalent memory as an infection episode and further expanding
399 previously established responses. These data further suggest that booster shots, if needed to address
400 antibody-escape to Omicron and other variants, will not substantially alter the repertoires of
401 established anti-spike T cell memory.
402
403 Our data have also provided a useful confirmation of the specific sequence features of several
404 SARS-CoV-2 epitope-specific responses. The generation of monoclonal T cell lines that can be
405 used to rapidly survey variant peptides provides an analogous tool as a monoclonal antibody for
406 characterizing antibody escape mutations. Here, we were able to show subtle variations in the loss
407 of recognition by multiple TCR lines recognizing the same epitope. These tools can be used to
408 screen emerging variants of concern and also predict mutations that might lead to relevant epitope
409 escape.
410
411 Our study has several limitations that should be considered. First, we focus on comparisons
412 between T cells specific for a pre-selected set of $CD8^+$ epitopes previously identified in large
413 epitope discovery studies[54]. This set of epitopes, although considerable in size given the nature of
414 our experiments, does not necessarily cover all immunodominant responses, and may also exclude
415 novel epitopes induced only by vaccination (though to date none have been reported). Furthermore,
416 the epitopes chosen are presented on a limited subset of HLA-alleles that, while abundant in
417 populations of European ancestry, are less representative of other populations. Additional epitope
418 discovery studies of SARS-CoV-2 and other clinically relevant pathogens covering more HLA
419 alleles from cohorts of diverse ancestry are important to overcome current biases in the literature
420 and integral for fully elucidating the complex interactions between genotype, phenotype, and

421 environment on the immune response. Secondly, we were only able to analyze a relatively small
422 number of breakthrough infection cases. Our data suggest that, going forward, it will be important
423 to more exhaustively profile the epitope-specific responses of individuals who experience
424 breakthrough infections, particularly by obtaining prospective samples after vaccination but prior
425 to infection.

426 In addition, we only had access to PBMC samples, which do not allow study of the distinct
427 features of the cellular response at the site of infection. Particularly in breakthrough infections, if
428 differential trafficking of memory cells to the airways occurred, it may bias our interpretation of
429 the observed response. Lastly, the variation in our sampling times across all subgroups may
430 introduce additional noise due to active T cell response dynamics. More regular and frequent
431 sampling in a larger cohort of fully vaccinated individuals will facilitate a more exhaustive
432 understanding of the correlates of protection from SARS-CoV-2 infection and the mechanisms
433 underlying breakthrough infection.
434

Online methods

Human cohort

The St. Jude Tracking of Viral and Host Factors Associated with COVID-19 study (SJTRC, NCT04362995) is a prospective, longitudinal cohort study of St. Jude Children's Research Hospital adult (≥18 years old) employees. The St. Jude Institutional Review Board approved the study. Participants provided written informed consent prior to enrollment and completed regular questionnaires about demographics, medical history, treatment, and symptoms if positively diagnosed with SARS-CoV-2 by PCR. Study data are collected and managed using REDCap electronic data capture tools hosted at St. Jude[55,56]. Participants were screened for SARS-CoV-2 infection by PCR weekly when on the St. Jude campus. For this study, we selected a cohort of 55 individuals, 16 of which had never tested positive for SARS-CoV-2 (N1-N16), and 39 of which were diagnosed as SARS-CoV-2 positive with a PCR test and recovered from mild disease (R1-R30, breakthrough B1-B9) during the study period. All individuals in this study received two doses of the Pfizer-BioNTech BNT162b2 mRNA vaccine. Vaccination data, including vaccine type and date administered, were obtained from the institutional database which required direct confirmation of vaccine administration records before data entry. Previously infected and naive vaccinated individuals (inf-vax2 and vax2) were sampled at similar time points after their vaccine regimen was complete (R1-R30: 45.5±2.8 SEM, range 25-81 days; N1-N16: 40.7±2.7 SEM, range 23-60 days). Finally, the individuals chosen for each group were of similar ages (R1-R30: 44.2±2.5 SEM, range 23-68 years; N1-N16: 44.1±3 SEM, range 29-73 years; B1-B9: 40.1±4.2 SEM, range 24-60 years). For this study, we utilized the convalescent blood draw for SARS-CoV-2 infected individuals (3-8 weeks post-diagnosis) and the post-vaccination samples (3-8 weeks after completion of the vaccine series). For breakthrough infections, we used the convalescent blood draw. An infection was considered a "breakthrough" if an individual tested positive for SARS-CoV-2 infection by PCR after receiving two doses of the Pfizer-BioNTech BNT162b2 vaccine. Blood samples were collected in 8 mL CPT tubes and separated within 24 hours of collection into cellular and plasma components then aliquoted and frozen for future analysis. Human cohort metadata can be found in Extended data Table 2.

466 **HLA typing**

467 High quality DNA was extracted from whole blood aliquots from each participant using the Zymo
468 Quick-DNA 96 Plus Kit (Qiagen). DNA was quantified on the Nanodrop (Thermo Scientific).
469 HLA typing of each participant was performed using the AllType NGS 11-Loci Amplification Kit
470 (One Lambda; Lot 013) according to manufacturer's instructions. Briefly, 50 ng DNA was
471 amplified using AllType NGS 11-Loci amplification primers. The amplified product was then
472 cleaned and quantified on the Qubit 4.0 (Invitrogen). Library preparation of purified amplicons
473 was carried out as described in the protocol, and the AllType NGS Index Flex Kit (Lot 011) was
474 used for barcoding and secondary amplification. Purified, barcoded libraries were quantified using
475 the Qubit DNA HS kit (Invitrogen) and pooled according to the One Lambda Library Pooling
476 table. Pools of up to 48 libraries were then purified and quantified on the TapeStation D5000
477 (Agilent) before sequencing on a full MiSeq lane at 150x150bp following manufacturer's
478 sequencing specifications. HLA types were called using the TypeStream Visual Software from
479 One Lambda. HLA typing results can be found in Extended data Table 2.

480

481 **Dextramer generation and cell staining**

482 Peptides with >95% purity were ordered from Genscript and diluted in DMSO to 1 mM. pMHC
483 monomers (500 nM) were generated with easYmer HLA class I (A*01:01, A*02:01, A*24:02,
484 B*15:01, B*44:02) kits (Immunaware) according to the manufacturer's protocol. To generate
485 DNA-barcoded MHC-dextramers we used Klickmer technology (dCODE Klickmer, Immudex).
486 16.2 µL of HLA monomer (500 nM) were mixed with 2 µL barcoded dCODE-PE-dextramer to
487 achieve an average occupancy of 15 and incubated for at least 1 hour on ice prior to use. Individual
488 dextramer cocktails were prepared immediately before staining. Each cocktail had 1.5 µL of each
489 HLA-compatible barcoded MHC-dextramer-PE and 0.15 µL 100 µM biotin per dextramer pre-
490 mixed to block free binding sites. Samples were divided into 3 batches, and timepoints from the
491 same donor were always processed simultaneously. Donor PBMCs were thawed and resuspended
492 in 50 µL FACS buffer (PBS, 0.5% BSA, 2 mM EDTA). Cells were stained with 5 µL Fc-block
493 (Human TruStain FcX, Biolegend 422302) and a cocktail of dextramers for 15 minutes on ice.
494 After this a cocktail of fluorescently-labeled surface antibodies (2 µL of each: Ghost Dye Violet
495 510 Viability Dye, Tonbo Biosciences 13-0870-T100; anti-human CD3 FITC-conjugated
496 (Biolegend 300406, clone UCHT1), anti-human CD8 BV711-conjugated (Biolegend, 344734,

497 clone SK1)) and TotalSeq-C antibodies (1 µL anti-human CCR7 (Biolegend 353251), 1 µL anti-
498 human CD45RA (Biolegend 304163)) and 2 µL of TotalSeq-C anti-human Hashtag antibodies 1-
499 10 (Biolegend 394661, 394663, 394665, 394667, 394669, 394671, 394673, 394675, 394677,
500 394679) were added. Samples were incubated for 30 minutes on ice. Single, Live, CD3-positive,
501 CD8-positive, dextramer-positive cells were sorted into RPMI (Gibco) containing 10% FBS and
502 1% penicillin/streptomycin using a Sony SY3200 cell sorter. Sorted cells were immediately loaded
503 into a 10x reaction. Chromium Next GEM Single-Cell 5' kits version 2 (10x Genomics PN:
504 1000265, 1000286, 1000250, 1000215, 1000252 1000190, 1000080) were used to generate GEX,
505 VDJ and Cite-Seq libraries according to the manufacturer's protocol. Libraries were sequenced on
506 Illumina NovaSeq at 26x90bp read length.
507
508 **Single-cell RNAseq data analysis**
509 Raw data was processed with Cell Ranger version 6.0.0 (10X Genomics). Three batches were
510 subsequently combined using the aggregate function with default parameters. Resulting GEX
511 matrices were analysed with the Seurat R package version 4.0.4 [57]. Following standard quality
512 control filtering, we discarded low quality cells (nFeatures <200 or >5000, MT% >5%) and
513 eliminated the effects of cell cycle heterogeneity using the CellCycleScoring and ScaleData
514 functions. Next, we identified 2,000 variable gene features. Importantly, we excluded TCR/Ig
515 genes from variable features, so that the gene expression clustering would be unaffected by T cell
516 clonotype distributions. Next, we removed all non-CD8 cells from the data as well as cells labeled
517 with antibody hashtag #1 (Biolegend 394661) in batch 3, which were used solely as carrier cells
518 for the 10X reaction. Clusters were defined with the resolution parameter set to 0.5. Differentially
519 expressed genes between clusters were identified using the Seurat FindAllMarkers function with
520 default parameters. Differentially expressed genes for 11 resulting clusters can be found in
521 Extended data Table 3. R scripts for the final Seurat object generation can be found on GitHub
522 (https://github.com/pogorely/COVID_vax_CD8).
523
524 **Donor and epitope assignment using feature barcodes**
525 Cells were processed in 6 batches with each batch making a separate 10X Chromium reaction. In
526 each batch, individual PBMC samples were uniquely labeled with a combination of DNA-
527 barcoded hashing antibody (TotalSeq-C anti-human Hashtag antibodies 1-10, Biolegend) and a set

528 of DNA-barcoded MHC-multimers. We attributed a cell to a certain hashtag if more than 50% of
529 UMIs derived from hashing antibodies matched that hashtag. Cells specific to certain dextramers
530 were called similarly: we required more than 30% of dextramer-derived UMIs to contain a
531 dextramer-specific barcode, and if multiple dextramers passed this threshold the cell was
532 considered specific to both. If the most abundant dextramer barcode per cell was ≤ 3 UMIs, we
533 did not assign any epitope specificity to it. Cells were assigned to donors using a combination of
534 hashing antibody and dextramer barcode. TCRα and TCRβ sequences were assembled from
535 aggregated VDJ-enriched libraries using the CellRanger (v. 6.0.0) vdj pipeline. For each cell we
536 assigned the TCRβ and TCRα chain with the largest UMI count. The R script performing feature
537 barcode deconvolution, GEX and TCR join is available on Github
538 (https://github.com/pogorely/COVID_vax_CD8) as well as the resulting Extended data Table 4.
539

540 **TCR repertoire analysis**

541 T cell clones were defined as groups of cells from the same donor with identical nucleotide
542 sequences of both CDR3α and CDR3β (see Extended data Table 5 for unique T cell clones). To
543 correct erroneous or missing dextramer assignments for individual cells within a clone we assign
544 each T cell a specificity of the majority of cells from this clone. To measure the distance between
545 TCR α/β clonotypes and plot logos for dominant motifs we used the TCRdist algorithm
546 implementation and plotting functions from *conga* python package[58]. Sequence similarity network
547 analysis and visualizations were performed with the *igraph* R package[59] and *gephi* software[60]. We
548 exclude top 1% of vertices and edges with largest betweenness centrality values (which are likely
549 to occur due to cell doublets or artifacts of scTCR sequencing) to filter out a small number of
550 spurious connections between motif clusters A TCR motif cluster is then defined as a connected
551 component on a similarity network. TCRβ repertoire diversity calculation was performed using
552 normalized Shannon entropy $-(\sum_{i=1}^{n} p_i log_2(p_i))/log_2(n)$, where n is a total number of unique
553 TCRβ clonotypes, and *pi* is a frequency of *i-th* TCRβ clonotype (defined as the fraction of cells
554 with this TCRβ amongst all cells in a sample with defined TCRβ).
555

556 **Artificial antigen-presenting cells (aAPCs)**

557 A gBlock gene fragment encoding full-length HLA-A*01:01, HLA-A*02:01, HLA*A24:02 and
558 HLA-B*15:01 was synthesized by Genscript and cloned into the pLVX-EF1α-IRES-Puro

559 lentiviral expression vector (Clontech). Lentivirus was generated by transfecting HEK 293T cells
560 (American Type Culture Collection (ATCC) CRL-3216) with the pLVX lentiviral vector
561 containing the HLA insert, psPAX2 packaging plasmid (Addgene plasmid #12260), and pMD2.G
562 envelope plasmid (Addgene plasmid #12259). Viral supernatant was harvested and filtered
563 through a 0.45 µm SFCA syringe filter (Thermo Fisher) 24- and 48-hours post-transfection, then
564 concentrated using Lenti-X Concentrator (Clontech). K562 cells (ATCC CCL-243) were
565 transduced, then antibiotic selected for one week using 2 µg/mL puromycin in Iscove's Modified
566 Dulbecco's Medium (IMDM; Gibco) containing 10% FBS and 1% penicillin/streptomycin.
567 Surface expression of HLA was confirmed via flow cytometry using antibodies against HLA-A,
568 B, C (PE-conjugated, Biolegend 311406, clone W6/32).
569
570 **TCR-expressing Jurkat 76.7 cells**
571 TCR chains matching both the biggest clusters of Fig 4B, as well as the B15_NQK-specific
572 prediction from[52], were selected for Jurkat cell line generation (Extended data Table 6). TCRα and
573 TCRβ chains for the selected epitope-specific TCRs were modified to use murine constant regions
574 (murine TRAC*01 and murine TRBC2*01). A gBlock gene fragment was synthesized by
575 Genscript to encode the modified TCRα chain, the modified TCRβ chain, and mCherry, with all
576 three genes linked together by 2A sites. This sequence was cloned into the pLVX-EF1α-IRES-
577 Puro lentiviral expression vector (Clontech). Lentivirus was generated by transfecting HEK 293T
578 cells (ATCC CRL-3216) with the pLVX lentiviral vector containing the TCR-mCherry insert,
579 psPAX2 packaging plasmid (Addgene plasmid #12260), and the pMD2.G envelope plasmid
580 (Addgene plasmid #12259). Viral supernatant was harvested and filtered through a 0.45 µm SFCA
581 syringe filter (Thermo Fisher) 24- and 48-hours post-transfection, then concentrated using Lenti-
582 X Concentrator (Clontech). Jurkat 76.7 cells (a gift from Wouter Scheper; variant of TCR-null
583 Jurkat 76.7 cells that expresses human CD8 and an NFAT-GFP reporter) were transduced, then
584 antibiotic selected for 1 week using 1 µg/mL puromycin in RPMI (Gibco) containing 10% FBS
585 and 1% penicillin/streptomycin. Transduction was confirmed by expression of mCherry, and
586 surface TCR expression was confirmed via flow cytometry using antibodies against mouse TCRβ
587 constant region (PE-conjugated, Biolegend 109208, clone H57-597) and human CD3 (Brilliant
588 Violet 785-conjugated, Biolegend 344842, clone SK7).
589

590 **Intracellular cytokine staining functional assay**

591 Jurkat 76.7 cells expressing the B15_NQK-specific TCR ($2.5x10^5$) were co-cultured with HLA-
592 B*15:01 aAPCs ($2.5x10^5$) pulsed with 1 μM of either NQKLIANAF peptide from HKU1/OC43
593 common cold coronaviruses or NQKLIANQF peptide from SARS-CoV-2, 1 μg/mL each of anti-
594 human CD28 (BD Biosciences 555725) and CD49d (BD Biosciences 555501), brefeldin A
595 (GolgiPlug, 1 μL/mL; BD Biosciences 555029), and monensin (GolgiStop, 0.67 μL/mL; BD
596 Biosciences 554724). An unstimulated (CD28, CD49d, brefeldin A, monensin) and positive
597 control (brefeldin A, monensin, 1X Cell Stimulation Cocktail, PMA/ionomycin; eBioscience 00-
598 4970-93) were included in each assay. Cells were incubated for 6 hours (37 ºC, 5% CO_2), washed
599 twice with FACS buffer (PBS, 2% FBS, 1 mM EDTA), then blocked using human Fc-block (BD
600 Biosciences 564220) for 10 minutes at room temperature. The blocked cells were then stained with
601 1 μL Ghost Dye Violet 510 Viability Dye (Tonbo Biosciences 13-0870-T100) and a cocktail of
602 surface antibodies 1 μL each of anti-human CD8 (Brilliant Violet 785-conjugated, Biolegend
603 344740, clone SK1), anti-human CD3 (Brilliant Violet 421-conjugated, Biolegend 344834, clone
604 SK7), and anti-mouse TCRβ chain (PE-conjugated, Biolegend 109208) or APC/Fire750-
605 conjugated, Biolegend 109246), clone H57-597) for 20 minutes at room temperature. Surface-
606 stained cells were washed twice with FACS buffer, then fixed and permeabilized using the
607 Cytofix/Cytoperm Fixation/Permeabilization kit (BD Biosciences) according to the
608 manufacturer's instructions. Following fixation and permeabilization, cells were washed twice
609 with 1X Perm/Wash buffer and then stained with a cocktail of intracellular antibodies including
610 1.25 μL of anti-human IFNγ (Alexa Fluor 647-conjugated, Biolegend 502516, clone 4S.B3) and 1
611 μL anti-human CD69 (PerCP-eFluor710-conjugated, eBioscience 46-0699-42, clone FN50) at 4
612 ºC for 30 minutes. Cells were washed twice with 1X Perm/Wash buffer, and then were analyzed
613 by flow cytometry on a custom-configured BD Fortessa using FACSDiva software (Becton
614 Dickinson). Flow cytometry data were analyzed using FlowJo v. 10.7.1 software (TreeStar).
615 Responsiveness to peptide stimulation was determined by measuring frequency of NFAT-GFP,
616 IFNγ, and CD69 expression.

617

618 **Specificity validation of generated Jurkat cell lines**

619 Jurkat 76.7 cells expressing the epitope-specific TCRs ($1.5x10^5$) were co-cultured with aAPCs
620 ($1.5x10^5$) expressing the corresponding restricting HLA allele, and pulsed with 1 μM of cognate

621 SARS-CoV-2 peptide, 1 µg/mL each of anti-human CD28 (BD Biosciences 555725) and CD49d
622 (BD Biosciences 555501). An unstimulated (CD28, CD49d) and positive control (1X Cell
623 Stimulation Cocktail, PMA/ionomycin; eBioscience 00-4970-93) were included for each Jurkat
624 76.7 cell line. Cells were incubated for 8 hours (37 ºC, 5% CO_2) then washed with FACS buffer
625 (PBS, 2% FBS, 1 mM EDTA), resuspended in 50µL FACS buffer, and blocked using human Fc-
626 block (BD Biosciences 564220) for 10 minutes at room temperature. Cells were then stained with
627 1 µL Ghost Dye Violet 510 Viability Dye (Tonbo Biosciences 13-0870-T100) and a cocktail of
628 surface antibodies including 1 µL each of anti-human CD3 (Brilliant Violet 421-conjugated,
629 Biolegend 344834, clone SK7), 1 µL anti-human CD69 (PerCP-eFluor710-conjugated,
630 eBioscience 46-0699-42, clone FN50), and anti-mouse TCRβ chain (APC/Fire750-conjugated
631 (Biolegend 109246), clone H57-597). Cells were incubated for 20 minutes at room temperature
632 and then washed with FACS buffer. Cells were analyzed by flow cytometry on a custom-
633 configured BD Fortessa using FACSDiva software (Becton Dickinson). Flow cytometry data were
634 analyzed using FlowJo software version 10.7.1 (TreeStar). Responsiveness to peptide stimulation
635 was determined by measuring frequency of NFAT-GFP and CD69 expression.
636
637 To further test the specificity of generated Jurkat T cell lines we used dextramer staining with the
638 same dextramer reagents used for staining PBMCs (above). Jurkat cells were washed with FACS
639 buffer and resuspended in 50 µL. Cells were blocked with using human Fc-block (BD Biosciences
640 564220) and then stained with 1 µL of corresponding dextramer and 1 µL Ghost Dye Violet 510
641 Viability Dye (Tonbo Biosciences 13-0870-T100). A control Jurkat Cell line with known
642 irrelevant specificity was used as a negative control and was stained with all dextramer reagents
643 tested. All cells were stained for 40 minutes on ice. After the incubation cells were washed once
644 with FACS buffer. Cells were analyzed by flow cytometry on a custom-configured BD Fortessa
645 using FACSDiva software (Becton Dickinson). Flow cytometry data were analyzed using FlowJo
646 software version 10.7.1 (TreeStar).
647
648 **Tetramer generation and staining of cross-reactive Jurkat Cell line**
649 Biotinylated HLA-B*15-monomers loaded with NQKLIANQF (SARS-CoV-2) and
650 NQKLIANAF (CCCoV) versions of the peptide were tetramerised using TotalSeq-C-0951-PE-
651 Streptavidin (Biolegend 405261, 0.5 mg/mL) and TotalSeq-C-0956-APC-Streptavidin (Biolegend

652 405283, 0.5 mg/mL). 60 µL of HLA-monomers (500 nM) were mixed with 1 µL of PE-conjugated
653 (B15_NQKLIANQF) or APC-conjugated (B15_NQKLIANAF) streptavidin reagents and
654 incubated for 1 hour in the dark on ice. Jurkat 76.7 cells expressing the potentially cross-reactive
655 TCR were stained with 1 µL Ghost Dye Violet 510 Viability Dye (Tonbo Biosciences 13-0870-
656 T100) and 5 µL of each MHC-tetramer for 30 minutes on ice. Flow cytometry data were analyzed
657 using FlowJo software (TreeStar). Cross-reactivity of the Jurkat 76.7 T cell line was determined
658 by co-staining of the live cells with PE and APC-labeled MHC-tetramers.
659
660 **Recombinant SARS-CoV-2 proteins and ELISA**
661 Expression plasmids for the nucleocapsid (N) protein, spike protein, and the spike receptor binding
662 domain (RBD) from the Wuhan-Hu-1 isolate were obtained from Florian Krammer (Icahn School
663 of Medicine at Mount Sinai). Proteins were transfected into Expi293F cells using a ExpiFectamine
664 293 transfection kit (Thermo Fisher Scientific) as previously described[61]. Supernatants from
665 transfected cells were harvested and purified with a Ni-NTA column.
666 For hCoV and SARS-CoV-2 antibody detection, 384-well microtiter plates were coated overnight
667 at 4 ^{o}C, with recombinant proteins diluted in PBS. Optimal concentrations for each protein and
668 isotype were empirically determined to optimize sensitivity and specificity. SARS-CoV-2 spike
669 RBD was coated at 2 µg/mL in PBS. Full-length spike was coated at 2 µg/mL for IgG. N protein
670 was coated at 1 µg/mL. The spike proteins of hCoV-229E (Sino Biological, 40605-V08B), hCoV-
671 NL63 (Sino Biological, 40604-V08B), hCoV-HKU1 (Sino Biological, 40606-V08B), or hCoV-
672 OC43 (Sino Biological, 40607-V08B) were coated at 1 µg/mL for IgG detection. For all ELISAs,
673 plates were washed the next day three times with 0.1% PBS-T (0.1% Tween-20) and blocked with
674 3% Omniblok^{TM} non-fat milk (AmericanBio; AB10109-01000) in PBS-T for one hour. Plates were
675 then washed and incubated with plasma samples diluted 1:50 in 1% milk in PBS-T for 90 minutes
676 at room temperature. Prior to dilution, plasma samples were incubated at 56 ^{o}C for 15 minutes.
677 ELISA plates were washed and incubated for 30 minutes at room temperature with anti-human
678 secondary antibodies diluted in 1% milk in PBS-T: anti-IgG (1:10,000; Invitrogen, A18805). The
679 plates were washed and incubated at room temperature with OPD (Sigma-Alrich, P8287) for 10
680 minutes (for hCoV ELISAs) or SIGMAFAST OPD (Sigma-Alrich; P9187) for 8 minutes (for
681 SARS-CoV-2 ELISAs). The chemiluminescence reaction was stopped by addition of 3N HCl and
682 absorbances were measured at 490 nm on a microplate reader. The OD of each sample was

683 normalized to the OD of the same two positive control samples that were run on each plate. The
684 normalized OD is the percent ratio of the sample OD to the average OD of the positive controls
685 for the plate. For the SARS-CoV-2 ELISAs, we first screened samples from prior studies that were
686 collected before 2019 to identify the background level of the assay. Samples were considered
687 positive if the normalized OD was greater than two times the average of normalized ODs from all
688 SARS-CoV-2 negative samples in the SJTRC cohort (n=912). For the hCoV ELISAs, we screened
689 samples from a prior study that included very young children to identify samples to serve as
690 negative controls. Samples with a normalized OD greater than three times the average of the
691 normalized ODs for the negative controls were considered positive for the hCoV antigens.
692 Antibody levels for each donor can be found in the Extended data Table 2.
693
694 **Analysis of epitope mutations in SARS-CoV-2 variants**
695 We used the WHO definition of variant of concern and variant of interest updated January 10,
696 2022. A mutation was included in the analysis if it appears in at least 10% of the GISAID
697 (www.gisaid.org/hcov19-variants/, accessed on Dec 7 2021) isolates with the same Pango lineage
698 and appears in >1000 isolates from that Pango lineage (Rambaut et al. 2020). To analyze the
699 predicted binding of variant and wild type peptides, we used NetMHCpan 4.1b[47]. Results of this
700 analysis are in Extended data Table 7.
701
702 **Statistical analysis**
703 Statistical analysis was performed in R version 4.0.2. Wilcoxon signed-rank test was used to
704 compare paired pre-vaccination and post-vaccination samples; only donors with cells collected at
705 both timepoints were included in the test. Wilcoxon rank-sum test (Mann-Whitney U test) was
706 used to compare unpaired samples between pairs of study groups, Kruskal-Wallis H test was used
707 to test for difference between multiple study groups. Multiple testing correction was performed
708 using the Benjamini-Hochberg procedure. Ns not significant, * $p<0.5$, ** $p<0.01$, *** $p<0.001$
709
710 **Data and code availability**
711 Code required to reproduce source data for figures is available on GitHub:
712 https://github.com/pogorely/COVID_vax_CD8. All data produced in the study is available as

supplementary files. Raw sequencing data was deposited to Short Read Archive acc. PRJNA744851.

Acknowledgements

We thank all the donors who volunteered for the SJTRC study, Phil Bradley and Stefan Schattgen for their consultations on TCRdist and conga algorithms, Greig Lennon from St. Jude Immunology flow core for his help with FACS. This work was funded by ALSAC at St. Jude, the Center for Influenza Vaccine Research for High-Risk Populations (CIVR-HRP) contract number 75N93019C00052 (S.S-C, P.G.T), the St. Jude Center of Excellence for Influenza Research and Surveillance (S.S-C, M.A.M, P.G.T), HHSN272201400006C, 3U01AI144616-02S1 (P.G.T, M.A.M, S.S-C), and R01AI136514 (P.G.T).

Author Contributions

Conceptualization: A.A.M, M.V.P, E.K.A, J.C.C., P.G.T. Formal analysis: A.A.M, M.V.P, A.M.K, J.C.C, M.A.M, J.H.E, X.Z, K.V, G.W. Investigation: A.A.M., M.V.P, A.M.K, C-H.C, R.C.M, M.A.M, J.W, J.E., C-Y.L, D.B, S.T, P.K, D.D. S.M, S.R.O. Methods development: A.A.M, M.V.P, J.C.C., A.M.K, C-Y.L, S.S-C, M.A.M. Resources: S.S-C, M.A.M, P.T, J.H.E., J.W. Data and sample curation: J.W, J.H.E, E.K.A, J.C.C., K.J.A, SJTRC Study Team. Writing, original draft: A.A.M. and M.V.P. Writing, review, and editing: A.A.M, M.V.P, A.M.K, E.K.A, J.C.C, J.W, M.A.M, P.G.T. Visualization: A.A.M., A.M.K. Supervision: P.G.T. Funding Acquisition: P.G.T.

Competing interests

P.G.T has consulted or received honorarium and travel support from Illumina and 10X. P.G.T. serves on the Scientific Advisory Board of Immunoscape and Cytoagents.

744 **Extended data**

745 **Extended data Table 1.** SARS-CoV-2 derived $CD8^+$ epitopes used for MHC-multimer
746 generation.

747 **Extended data Table 2**. Study participant metadata.

748 **Extended data Table 3.** Differentially expressed genes for GEX clusters of epitope-specific CD8+
749 T cells.

750 **Extended data Table 4.** Epitope-specific $CD8^+$ T cells GEX clusters, TCR and epitope specificity.

751 **Extended data Table 5.** Unique epitope-specific $CD8^+$ αβTCR clonotypes.

752 **Extended data Table 6:** TCR amino acid sequences used for generation of TCR-expressing Jurkat
753 cell lines

754 **Extended data Table 7.** Mutations in studied epitopes from SARS-CoV-2 variants.

755

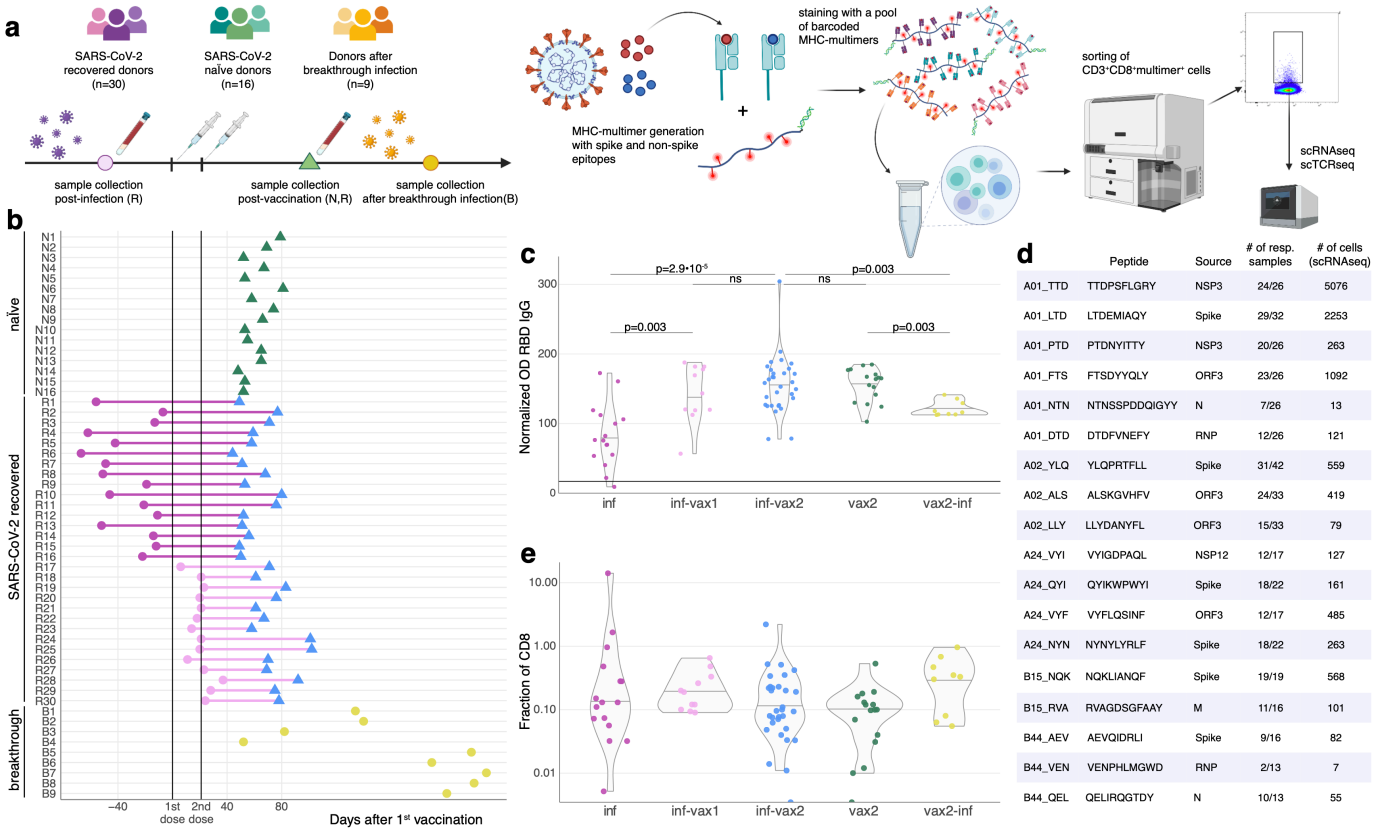

	Peptide	Source	# of resp. samples	# of cells (scRNAseq)
A01_TTD	TTDPSFLGRY	NSP3	24/26	5076
A01_LTD	LTDEMIAQY	Spike	29/32	2253
A01_PTD	PTDNYITTY	NSP3	20/26	263
A01_FTS	FTSDYYQLY	ORF3	23/26	1092
A01_NTN	NTNSSPDDQIGYY	N	7/26	13
A01_DTD	DTDFVNEFY	RNP	12/26	121
A02_YLQ	YLQPRTFLL	Spike	31/42	559
A02_ALS	ALSKGVHFV	ORF3	24/33	419
A02_LLY	LLYDANYFL	ORF3	15/33	79
A24_VYI	VYIGDPAQL	NSP12	12/17	127
A24_QYI	QYIKWPWYI	Spike	18/22	161
A24_VYF	VYFLQSINF	ORF3	12/17	485
A24_NYN	NYNYLYRLF	Spike	18/22	263
B15_NQK	NQKLIANQF	Spike	19/19	568
B15_RVA	RVAGDSGFAAY	M	11/16	101
B44_AEV	AEVQIDRLI	Spike	9/16	82
B44_VEN	VENPHLMGWD	RNP	2/13	7
B44_QEL	QELIRQGTDY	N	10/13	55

Figure 1. Measuring CD8$^+$ T cell epitope-specific responses after diverse SARS-CoV-2 exposures. a. Study design. Selected spike and non-spike SARS-CoV-2 T cell epitopes were loaded on recombinant biotinylated MHC-monomers. Resulting peptide-MHC complexes were polymerized using fluorescently labeled and DNA-barcoded dextran backbones. Next, we stained PBMC samples with pools of MHC-multimers, isolated bound cells using FACS, and performed scRNAseq, scTCRseq, and CITEseq using the 10X Genomics platform. **b.** Time of blood sampling for each donor is shown relative to the first dose of mRNA vaccine. **c. Anti-RBD IgG antibody levels in previously infected individuals increase after BNT162b2 vaccination.** Anti-RBD IgG levels in the plasma were determined by ELISA. The normalized OD is the percent ratio of the sample OD to the OD of the positive control for each plate. Plasma was collected from previously infected donors prior (purple, inf), after 1 vaccine dose (inf-vax1, pink), and after 2 vaccine doses (inf-vax2, blue); SARS-CoV-2 naive donors after the full vaccination (vax2, green), and donors that were infected after vaccination (breakthrough, vax2-inf, yellow). All comparisons were done with Mann-Whitney U test, p-values are reported after Benjamini-Hochberg correction. Central line on violin plots depicts the median. **d. List of SARS-CoV-2 epitopes used in this study and summary statistics for resulting epitope-specific response. e. Total frequency of MHC-dextramer-positive cells is similar in all studied groups** ($p>0.05$ for all pairwise comparisons, Mann-Whitney U test after multiple test correction). Percentage of MHC-multimer-positive cells from all CD8$^+$ T cells measured by flow cytometry is shown on a $\log_{10}$-scale. Central line on violin plots shows the median.

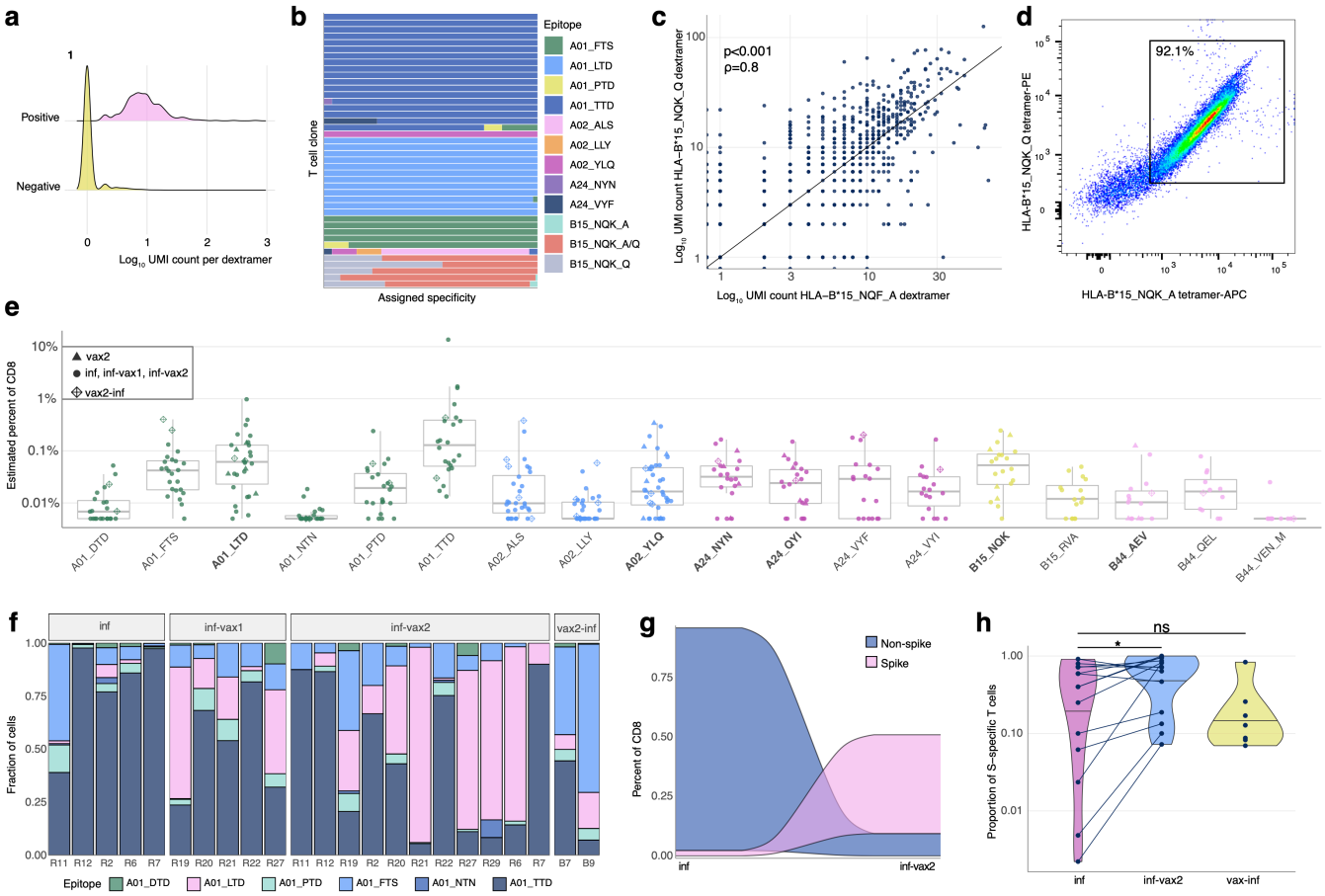

Figure 2. Magnitude, dynamics, and cross-reactivity of CD8$^+$ epitope-specific responses after diverse SARS-CoV-2 exposures. a. Antigen specificity of each T cell inferred from dextramer-barcode UMI counts. Representative distribution of the number of UMIs in cells called dextramer-positive (pink) and dextramer-negative (yellow). **b. T cells within a clone have largely consistent specificity assignments, except T cells that cross-react with common cold coronavirus epitopes (B15_NQK_A/B15_NQK_Q pair).** Each bar shows a fraction of cells of a given clonotype attributed to different dextramers. The 43 most abundant clones (more than 20 cells) are shown. **c. The correlation between the number of UMIs for B15_NQK_Q (SARS-CoV-2) and B15_NQK_A (OC43 and HKU1) dextramers (Spearman ρ=0.8, p<0.001). d. Cross-reactivity between HLA-B*15:01-NQK epitope variants confirmed *in vitro*.** Jurkat cell line expressing αβTCR identified from scTCRseq data binds pMHC multimers loaded with both SARS-CoV-2 and CCCoV variants of the epitope. **e. The magnitude of epitope-specific CD8$^+$ T cell responses.** Each point depicts an estimated frequency of epitope-specific T cells in a sample. Estimated frequency was calculated as a fraction of dextramer-specific T cells in scRNAseq results multiplied by bulk frequency of dextramer-stained CD8$^+$ cells of all CD8$^+$ cells measured by flow cytometry. Central line on boxplot shows the median. Epitopes from spike protein are in bold font. **f. Composition of HLA-A*01-restricted T cell response in HLA-A*01 positive donors.** Increasing proportion of spike-targeting T cells (pink) is observed after vaccination of infected individuals. **g. Boosting of spike-specific epitope fraction after vaccination (donor R6). h. Previously infected individuals have a higher proportion of spike-specific T cells after vaccination than before vaccination** (p=0.025, one-sided Wilcoxon signed-rank test). Spike T cell proportion (shown on a $\log_{10}$-scale) was calculated as a fraction of spike-specific T cells out of all CD8$^+$ epitope-specific T cells of a donor in scRNAseq data. Central line on the violin shows the median.

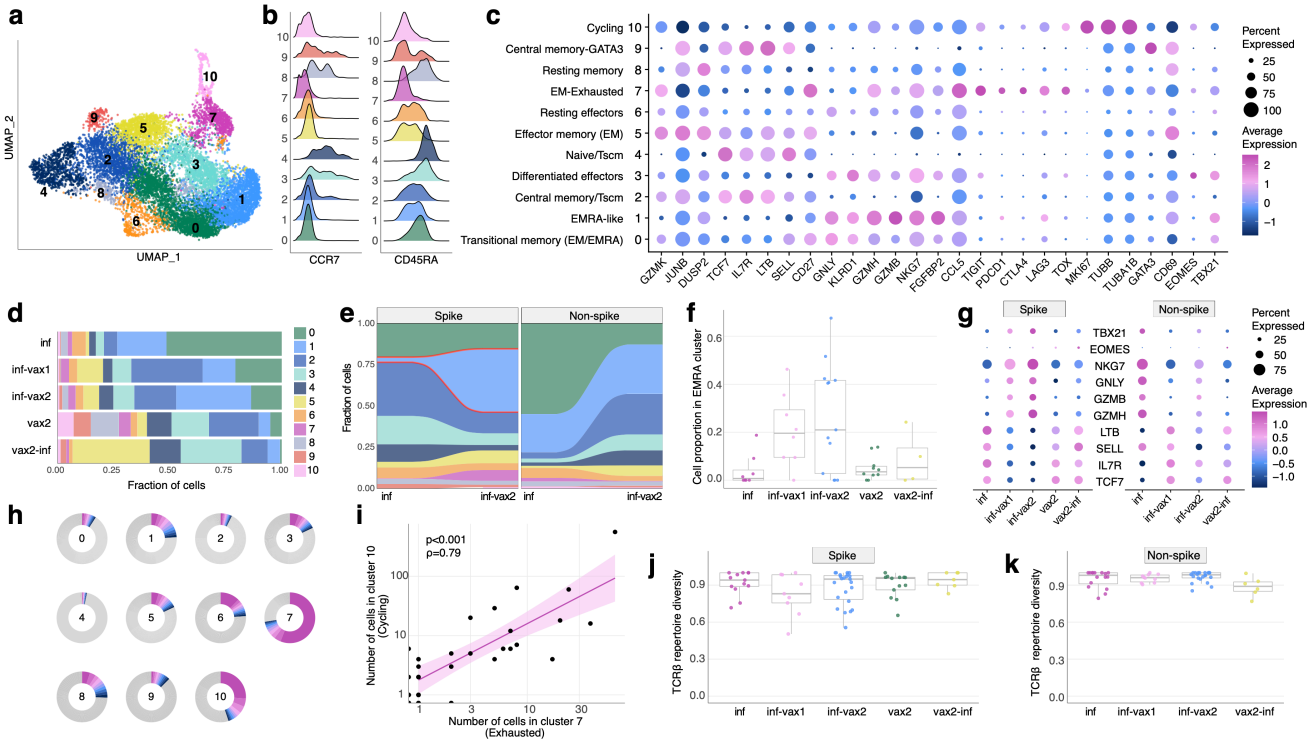

Figure 3. Phenotypic diversity of epitope-specific CD8$^+$ T cells after diverse SARS-CoV-2 exposures. a. UMAP (Uniform manifold approximation and projection) of all SARS-CoV-2 epitope-specific CD8 T cells based on gene expression (GEX). Color shows results of graph-based unsupervised clustering performed with the Seurat package. **b. Density plot of CCR7 and CD45RA surface expression (measured by CITE-seq) in GEX clusters. c. Bubble plot of representative differentially expressed genes for each cluster.** Size of the circle shows percentage of cells in a cluster expressing a certain gene, color scale shows gene expression level. **d. Distribution of epitope-specific T cells in gene expression clusters between study groups. e. Proportion of spike-specific T cells is significantly increased in cluster 1 after vaccination of previously infected individuals, compared to the pre-vaccination timepoint (p<0.0001, Fisher exact test). f. Proportion of spike-specific cells in EMRA (cluster 1) across study groups for samples with more than ten spike-specific cells (Kruskal-Wallis H test p=0.028).** Central line on boxplot shows the median. **g. Expression of classical cytotoxic and memory markers across study groups and T cell specificities.** Size of the circle shows percentage of cells in a cluster expressing a certain gene, color scale shows gene expression level. **h. Clone size distribution within GEX clusters.** Fractions of cells from 10 most abundant clonotypes in each cluster are shown with colors, all other clonotypes are shown in grey. **i. Number of cells in cluster 7 (Exhausted) and cluster 10 (Cycling) in samples are strongly correlated (Spearman ρ=0.79, p<0.001).** Shaded area shows 95% confidence interval for linear fit. **j-k. T cell repertoire diversity of spike (j) and non-spike specific repertoires across study groups** (p=0.63 for spike, p=0.17 for non-spike, Kruskal-Wallis H test)**.** Normalized Shannon entropy of TCRβ is plotted for samples with more than 3 unique TCRβ clonotypes. Central line on boxplot shows the median.

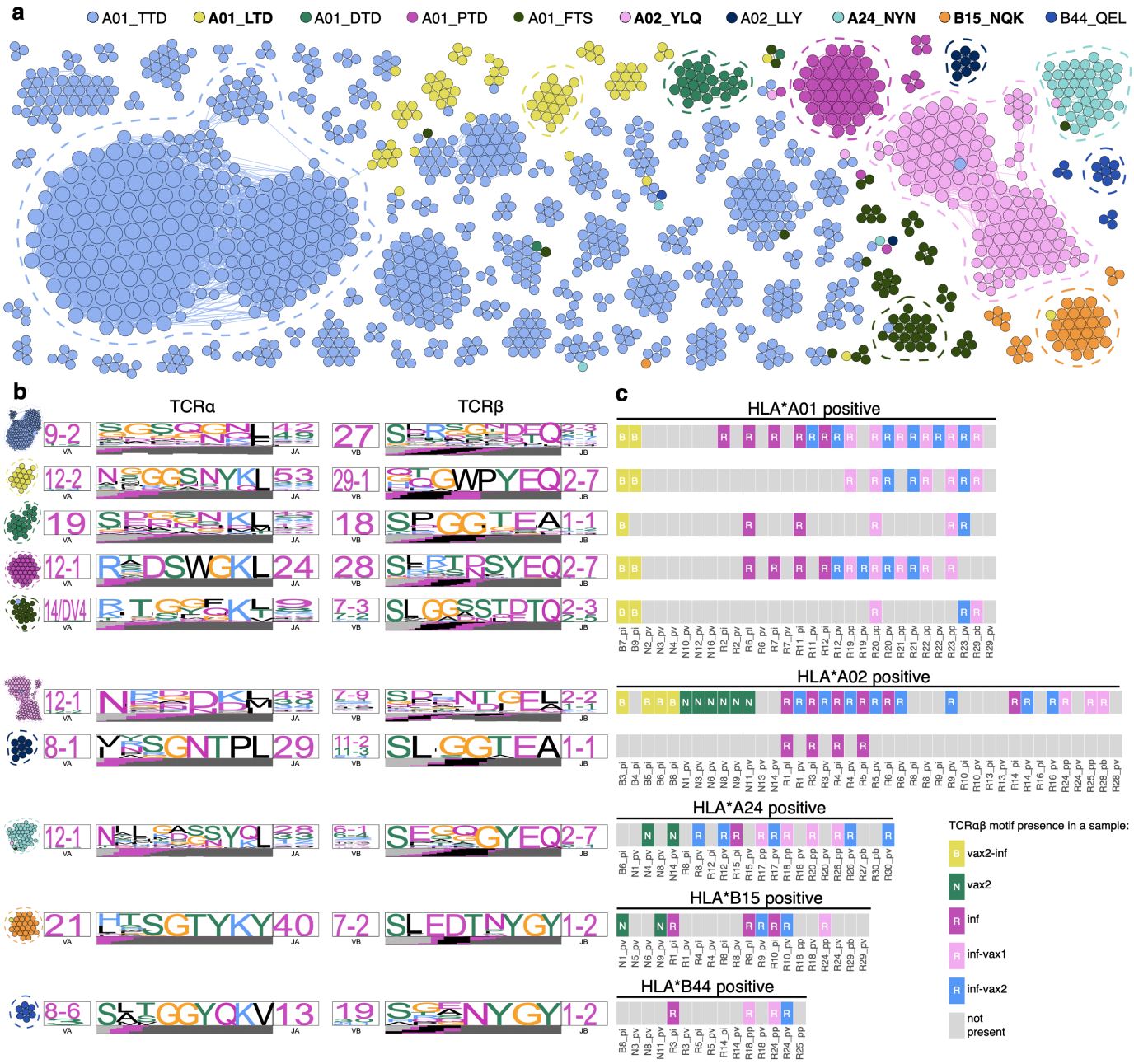

Figure 4. Diverse polyclonal repertoires of epitope-specific T cells after diverse SARS-CoV-2 exposures a. SARS-CoV-2 epitope-specific αβTCR amino acid clonotypes feature clusters of highly similar sequences with the same epitope specificity. Each node on a similarity network is a unique paired αβTCR amino acid sequence, and an edge connects αβTCRs with TCRdist less than 110. Each color represents a certain epitope specificity. Only clusters with more than two members are shown. Spike-derived epitopes are in bold font. **b. TCR amino acid sequence motifs of α and β chains (TCRdist logos) for the largest clusters of highly similar TCRs for each epitope (circled with dashed line on a). c. TCRs with the same sequence motifs are found across all study groups in a matching HLA-background.** Occurrence of TCR motifs on the left is shown for all HLA matching samples (rectangles on the plot). Grey rectangles represent samples lacking the TCR motif. The color of the rectangle that has a TCR motif corresponds to the sample group.

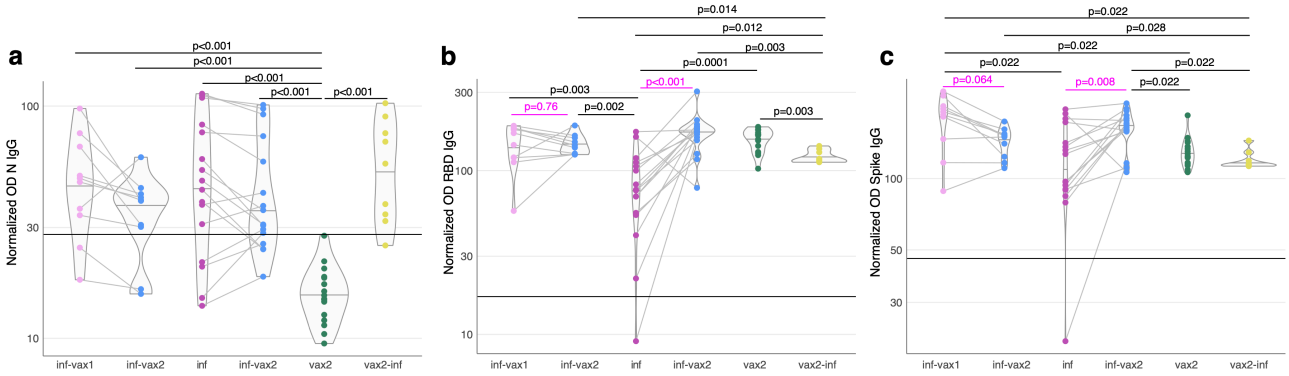

Extended data Fig. 1. Antibody levels across study groups. Plasma was tested by ELISA for IgG antibodies specific for (**a**) Nucleocapsid (N), (**b**) the receptor-binding domain (RBD) of the spike, (**c**) whole spike protein of SARS-CoV-2. Normalized ODs are the percent ratio of the sample OD to the OD of the positive control samples for each plate. The black horizontal line on the plots indicates the positivity threshold, which is two times the average of the normalized ODs for all SARS-CoV-2 negative samples in the cohort. P-values for Mann-Whitney U test after Benjamini-Hochberg multiple testing correction are reported. Donors sampled before and after mRNA vaccination are connected with a line. P-values (magenta) for paired samples were calculated with the Wilcoxon signed-rank test.

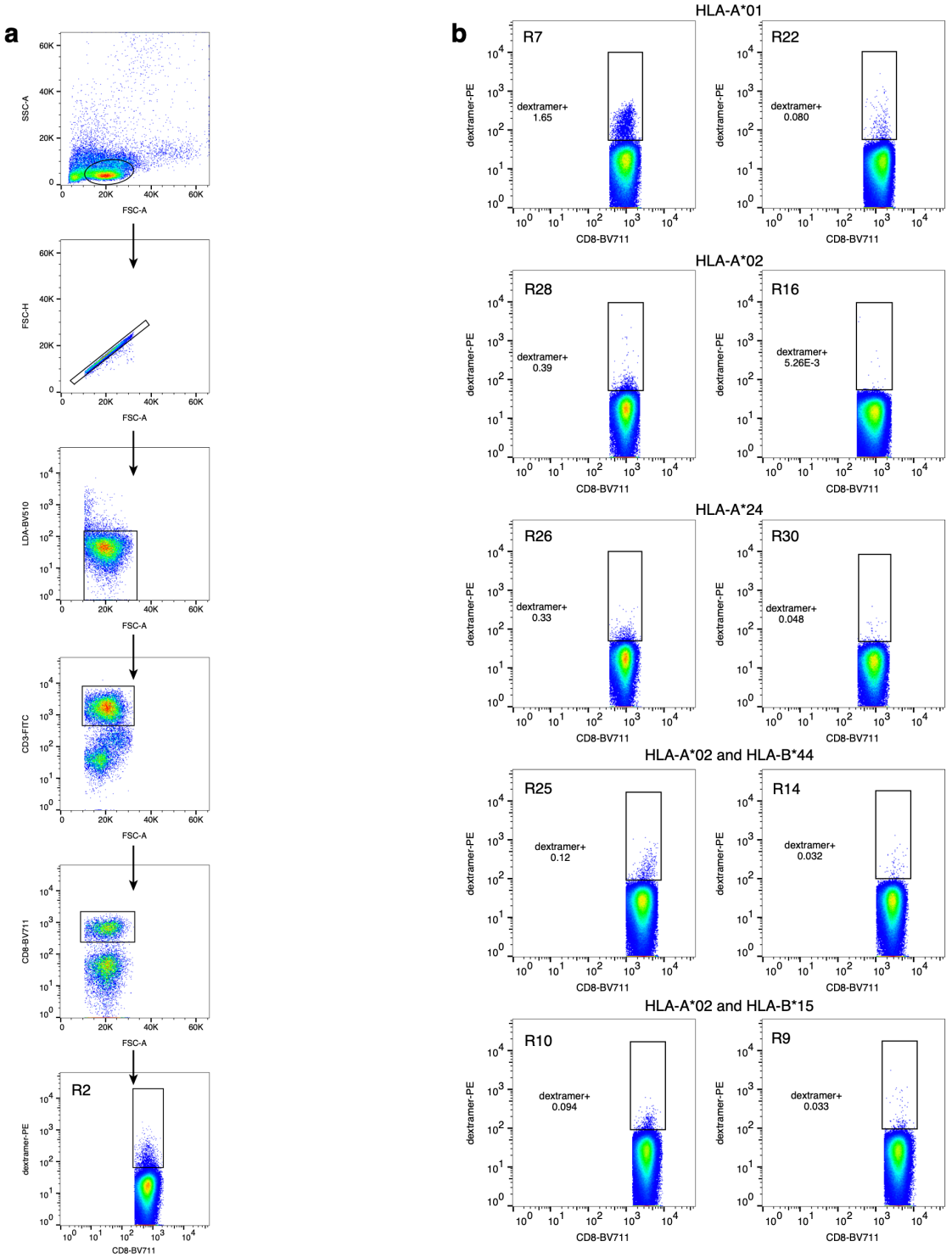

Extended data Fig. 2. a. Gating strategy for sorting of single live CD3$^+$CD8$^+$dextramer$^+$ cells. b. Representative flow plots for donors stained with the same dextramer pools, but showing different frequencies of single live CD3$^+$CD8$^+$dextramer$^+$ cells.

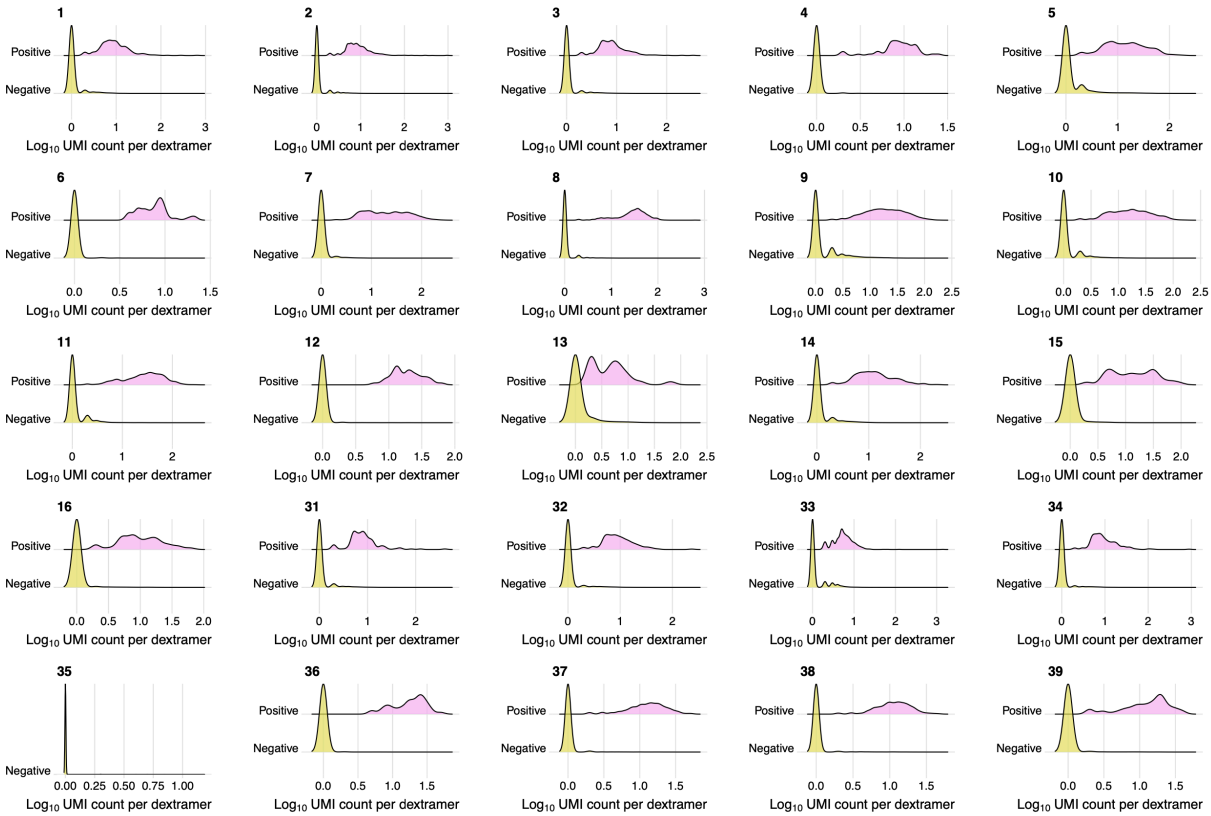

Extended data Fig. 3. **Dextramer assignment with feature barcodes**. Each subplot shows distribution of Log_{10} (# UMIs) for dextramers with certain feature barcodes in dextramer-negative (yellow) and dextramer-positive (pink) cells. Dextramer with barcode 35 B44_VEN_M did not have any specific cells.

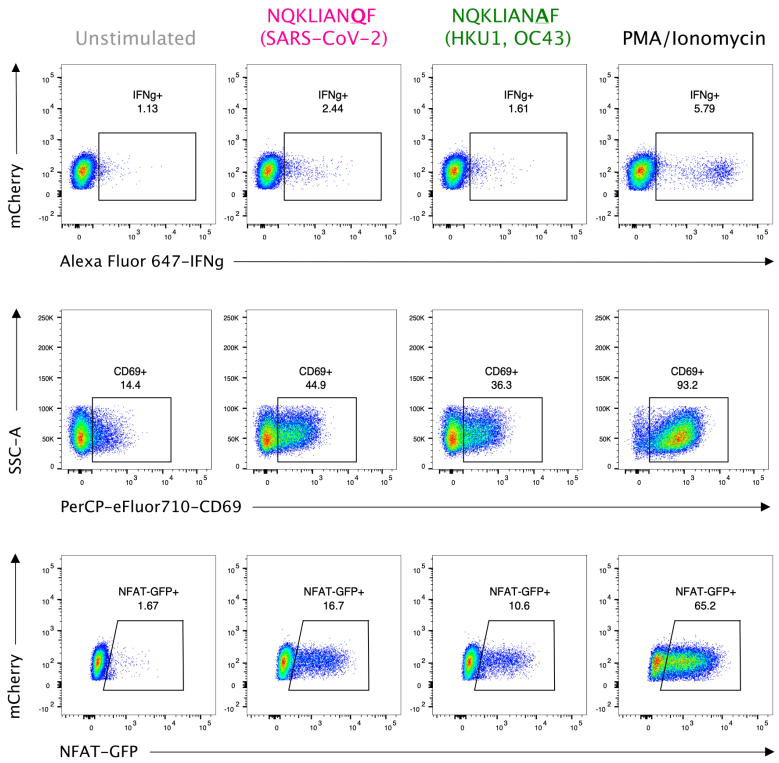

Extended data Fig. 4. **Peptide stimulation confirms cross-reactivity of B15_NQK αβTCR.** From left to right: unstimulated (negative control), NQKLIANQF (SARS-CoV-2) peptide stimulation, NQKLIANAF (OC43 and HKU1) peptide stimulation, PMA/Ionomycin (positive control). Top row: IFN-γ production by TCR-expressing Jurkats measured by intracellular cytokine staining. Middle row: CD69+ surface expression. Bottom row: NFAT-GFP reporter expression.

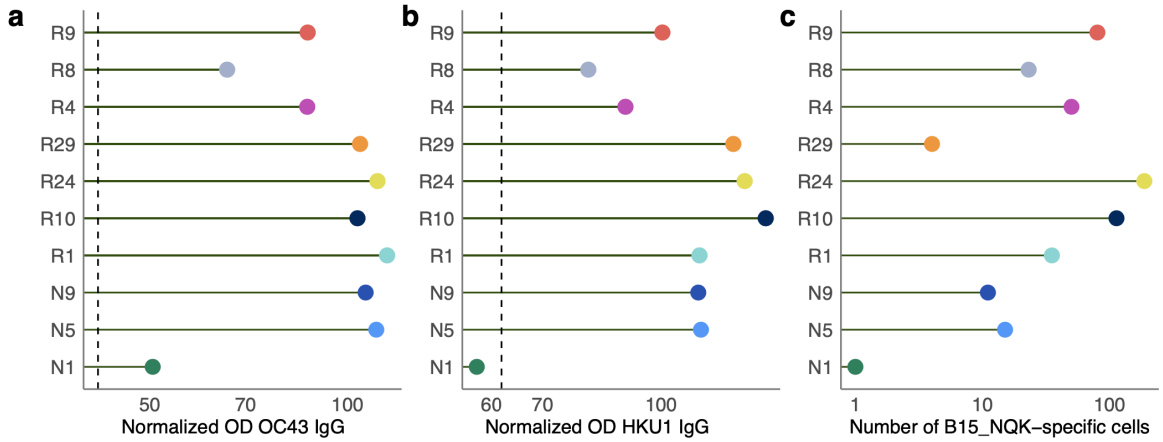

Extended data Fig. 5. **Antibody titers for CCCoV spike protein and number of B15_NQK cross-reactive cells in HLA-B*15:01^{+} donors.** Plasma collected from donors prior to infection or vaccination was tested by ELISA for IgG antibodies to the spike of **a,** hCoV-OC43 or **b,** hCoV-HKU1. The normalized ODs are the percent ratio of the sample OD to the OD of the positive control sample for each plate. The dashed line is the threshold for positivity, which is three times the average of the normalized OD for the negative control samples. **c,** The number of HLA-B*15:01-restricted epitope T cells after infection or vaccination (log-scale).

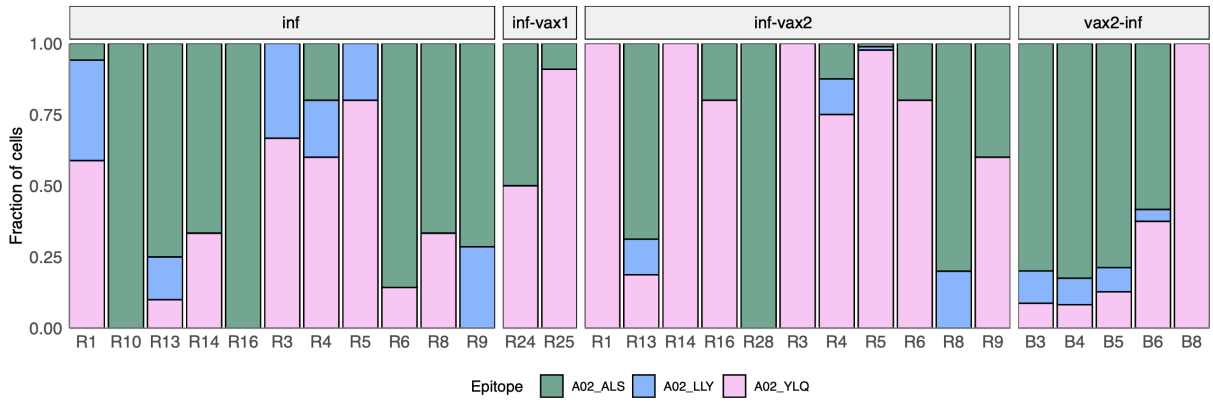

Extended data Fig. 6. Composition of HLA-A*02-restricted T cell response in HLA-A*02 positive donors. Increasing proportion of spike-targeting T cells (pink) is observed after vaccination of previously infected individuals.

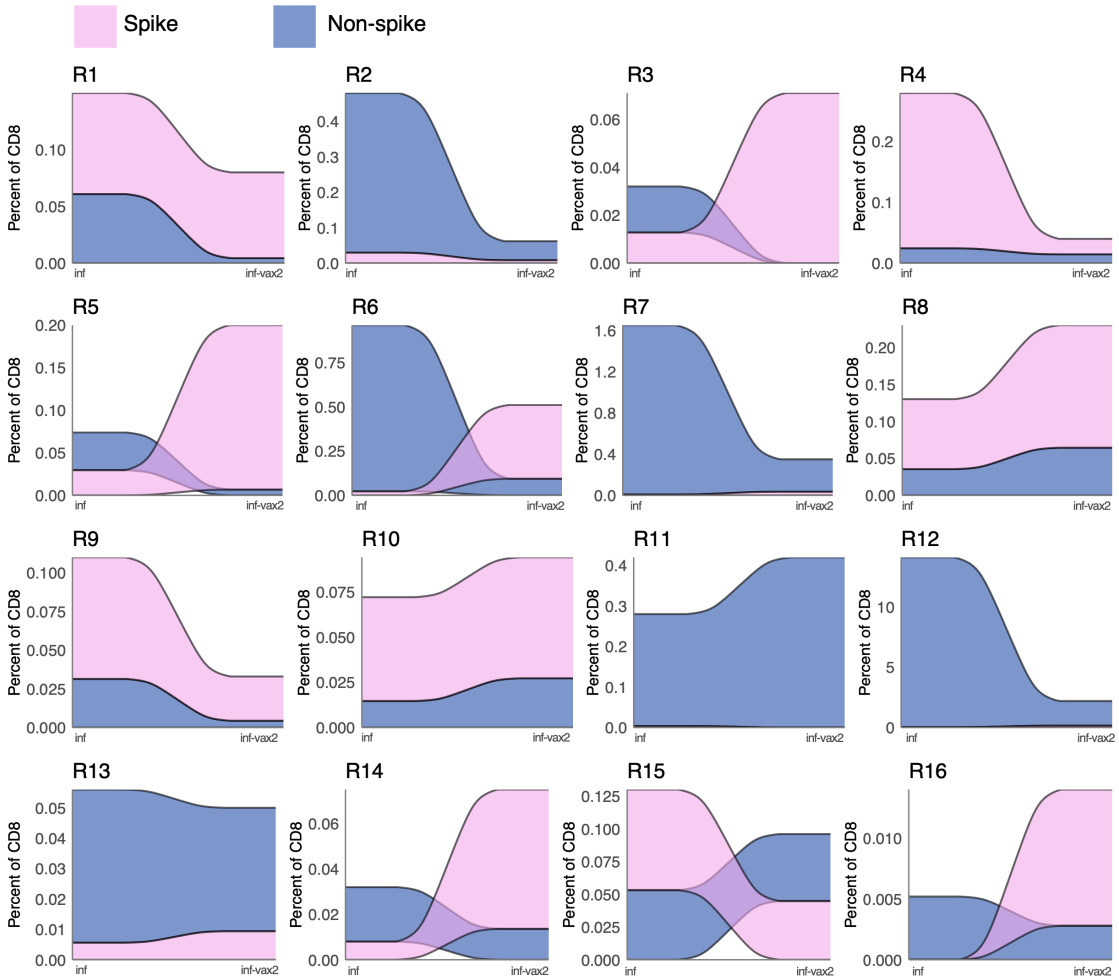

Extended data Fig. 7. Clonal dynamics of spike- and non-spike-specific T cell response for SARS-CoV-2 infected donors before and after two doses of BNT162b2. Each colored ribbon represents an estimated frequency of spike- (pink) or non-spike- (blue) specific T cells.

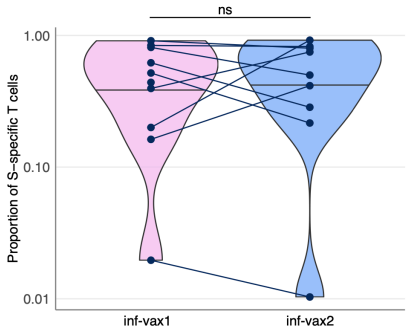

Extended data Fig. 8. SARS-CoV-2 infected individuals after the first and second BNT162b2 vaccine doses (inf-vax1 and inf-vax2) have the same proportion of spike-specific T cells (p=0.9, Wilcoxon signed-rank test). Spike T cell proportion was calculated as a fraction of spike-specific T cells out of all $CD8^+$ epitope-specific T cells of a donor in scRNAseq data.

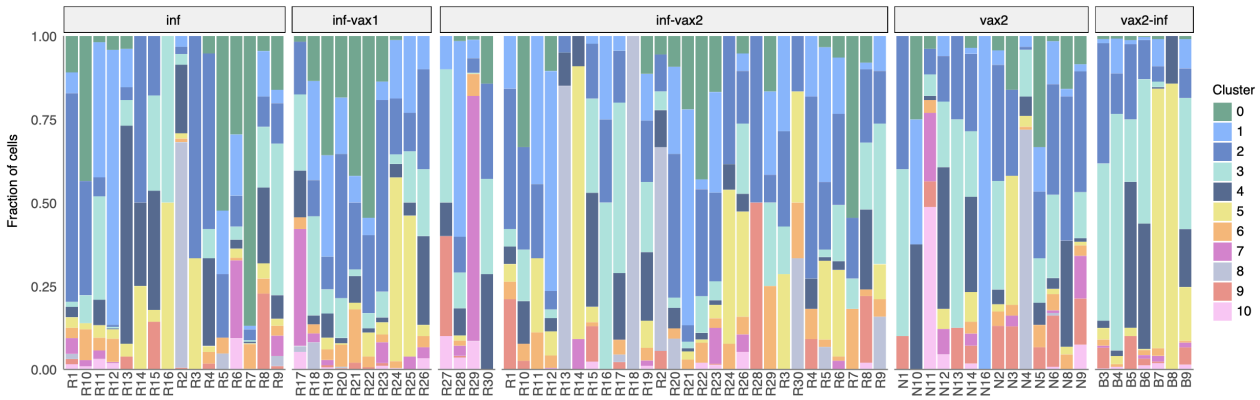

Extended data Fig. 9. GEX cluster distribution for each sample. Each colored bar represents a fraction of cells in a given GEX cluster.

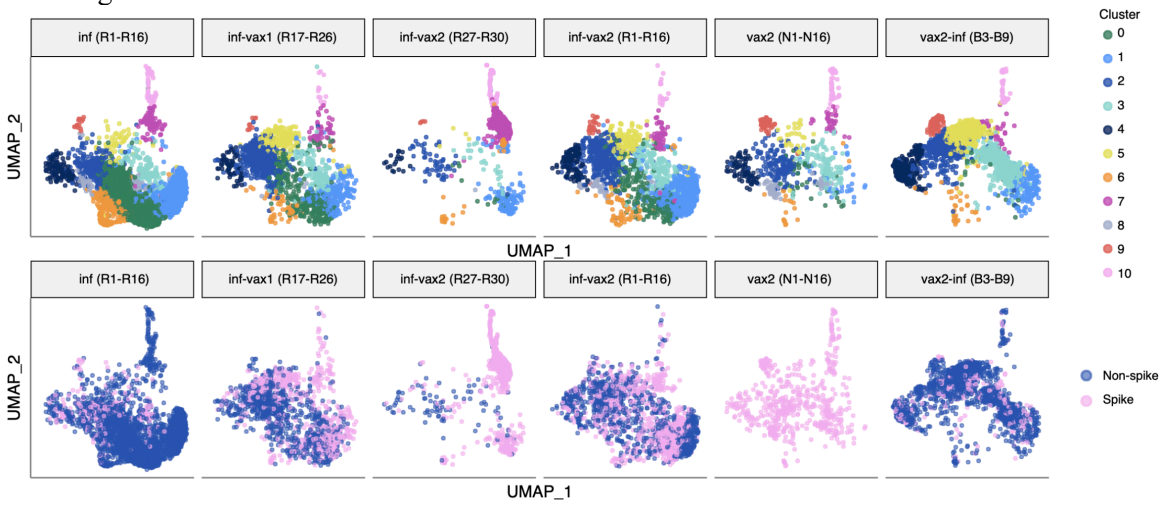

Extended data Fig. 10. UMAP visualization of cells clustered by similarity of GEX. Each subpanel shows cells from each study group. Top: cells colored by cluster. Bottom: cells colored by spike and non-spike specificity.

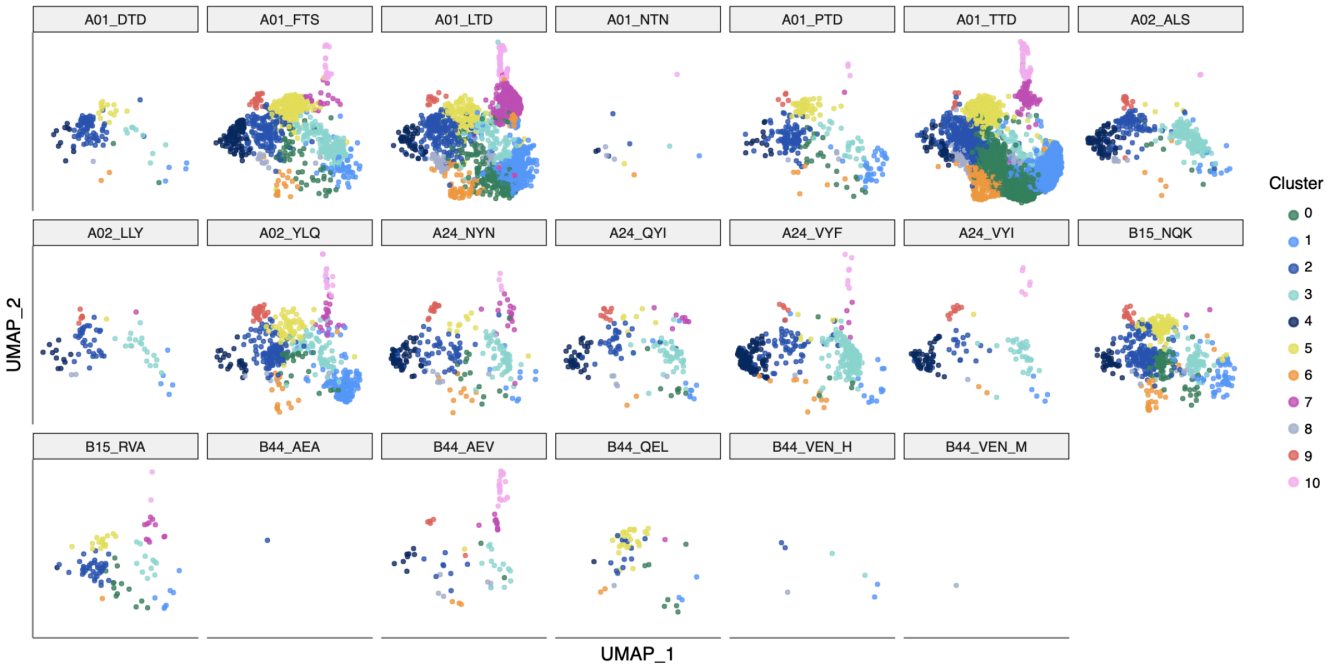

Extended data Fig. 11. UMAP visualization of cells clustered by similarity of GEX. Each subpanel shows cells specific for each of the tested epitopes.

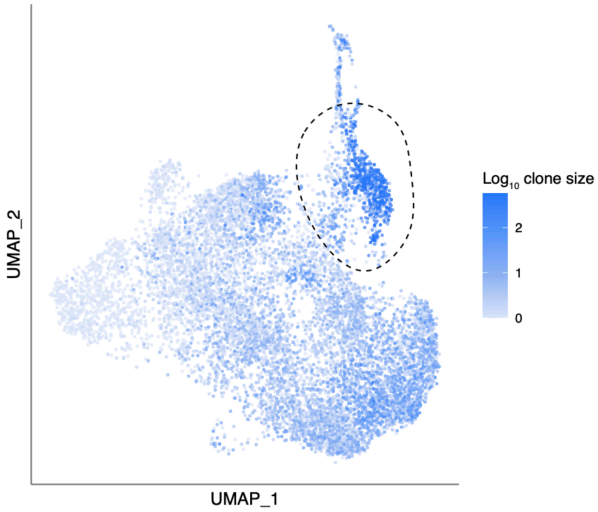

Extended data Fig. 12. "Exhausted" cluster 7 (circled) is enriched with cells from expanded clones. The color of each dot shows the size of the T cell clone (Log_{10} of number of cells) for each cell.

Figure S13

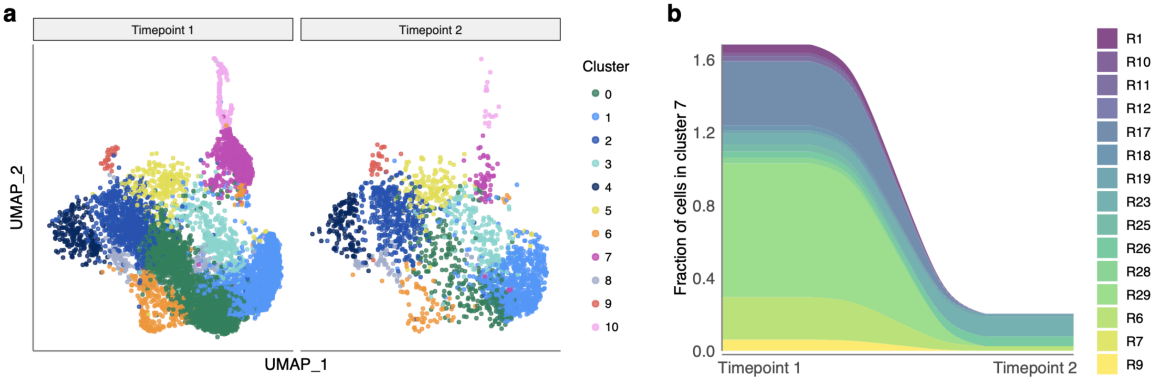

Extended data Fig. 13. Number of cells in the "exhausted" cluster (cluster 7) declines over time. a. UMAP visualization of cells clustered by similarity of GEX for donors sampled twice during the study (shapes connected with a line on Fig. 1b). Timepoint 1 corresponds to inf (R1-R16), inf-vax (R17-R30); timepoint 2 corresponds to inf-vax2 (R1-R30). **b. Fraction of cells in cluster 7 out of all cells.** Only donors with cells in cluster 7 on timepoint 1 are shown.

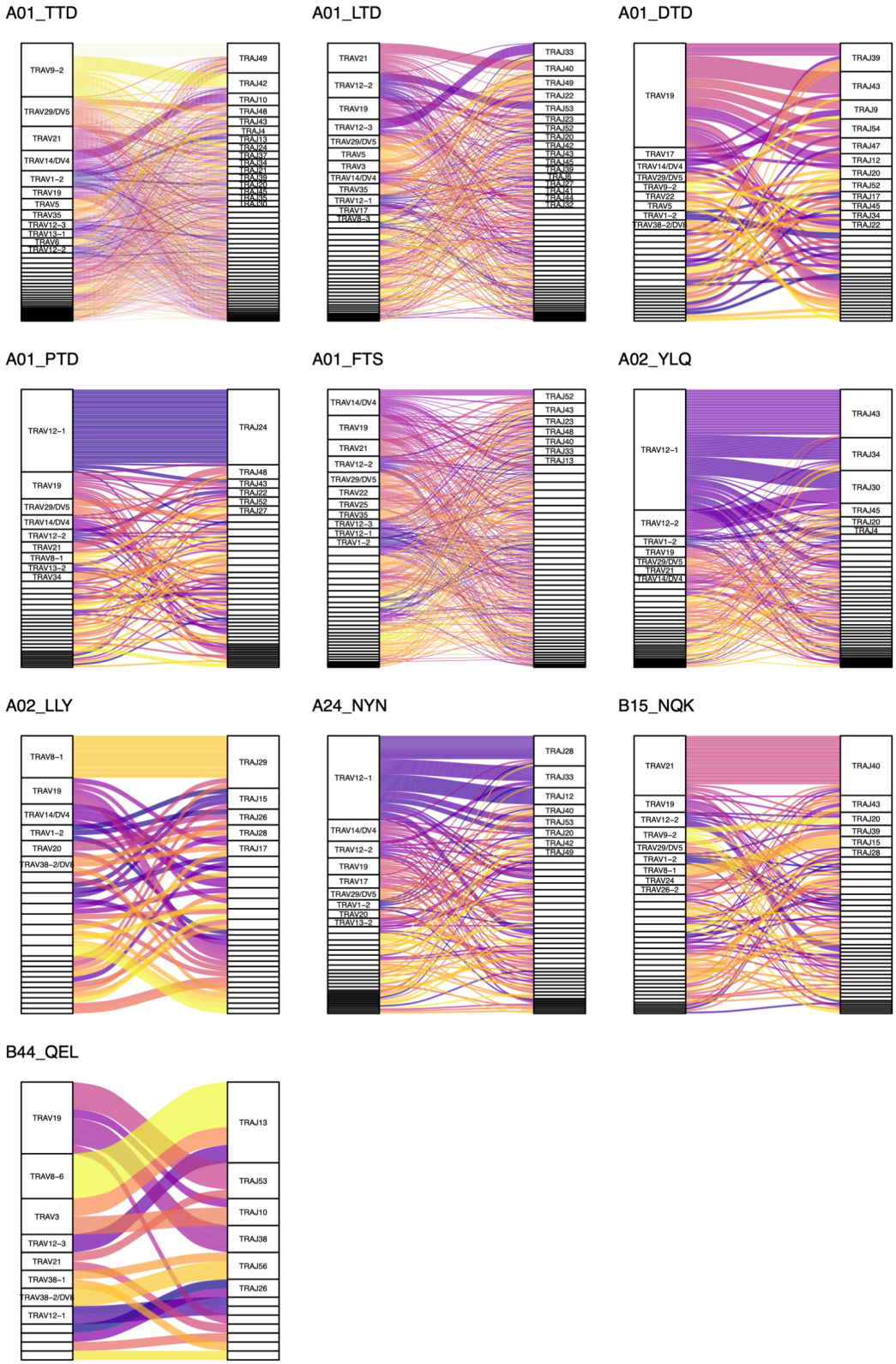

Extended data Fig. 14. VαJα-usage for selected epitopes. Height of each rectangle corresponds to the fraction of unique epitope-specific T cell clones expressing a given V- or J-segment in the TCRα. Ribbons show the frequency of VJ combinations.

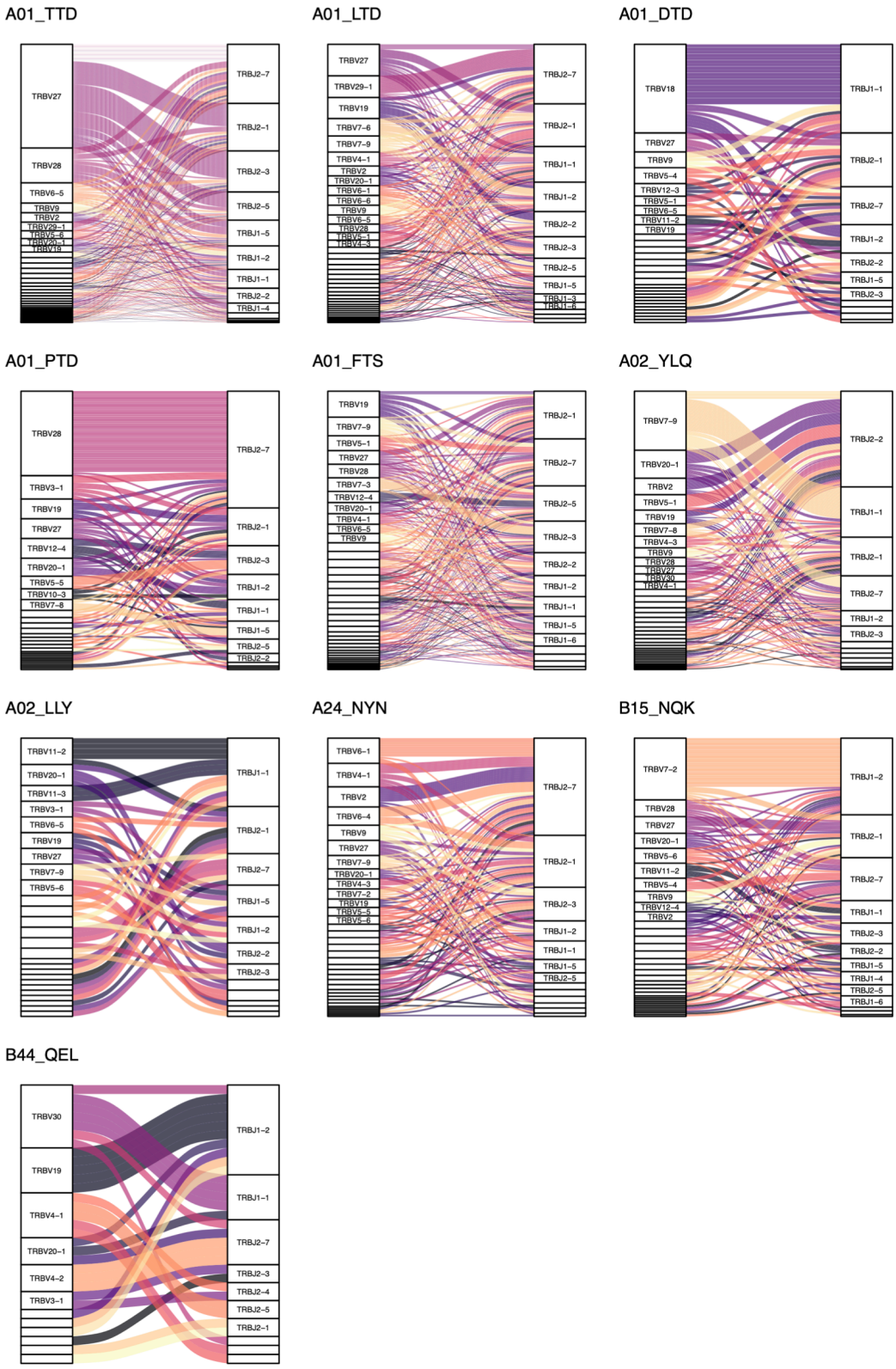

Extended data Fig. 15. VβJβ-usage for selected epitopes. Height of each rectangle corresponds to the fraction of unique epitope-specific T cell clones expressing a given V- or J-segment in the TCRβ chain. Ribbons show the frequency of VJ combinations.

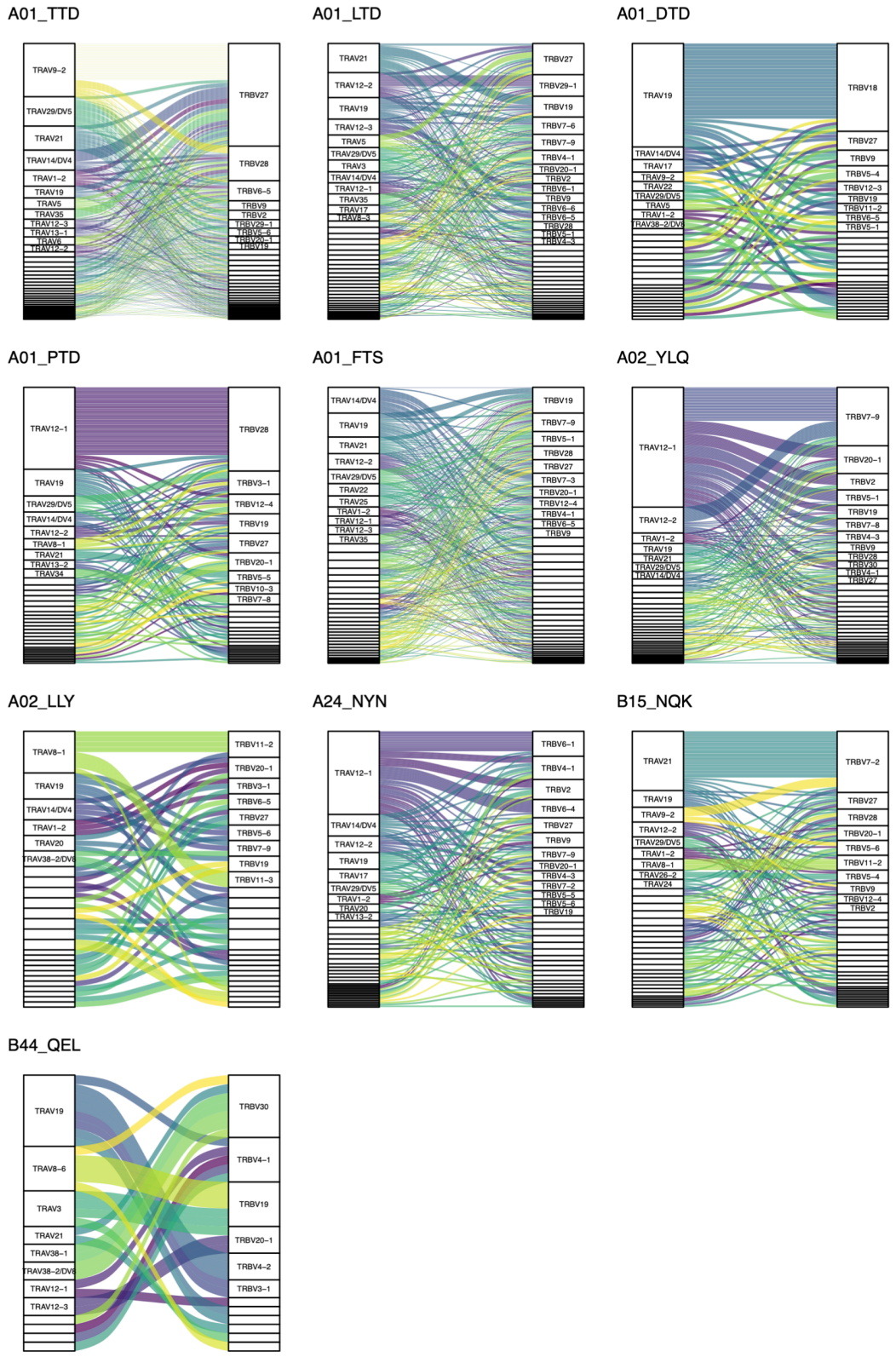

Extended data Fig. 16. Vα-Vβ pairings for selected epitopes. Height of each rectangle corresponds to the fraction of unique epitope-specific T cell clones expressing a given TRAV or TRBV segment. Ribbons show frequencies of TRAV-TRBV combinations.

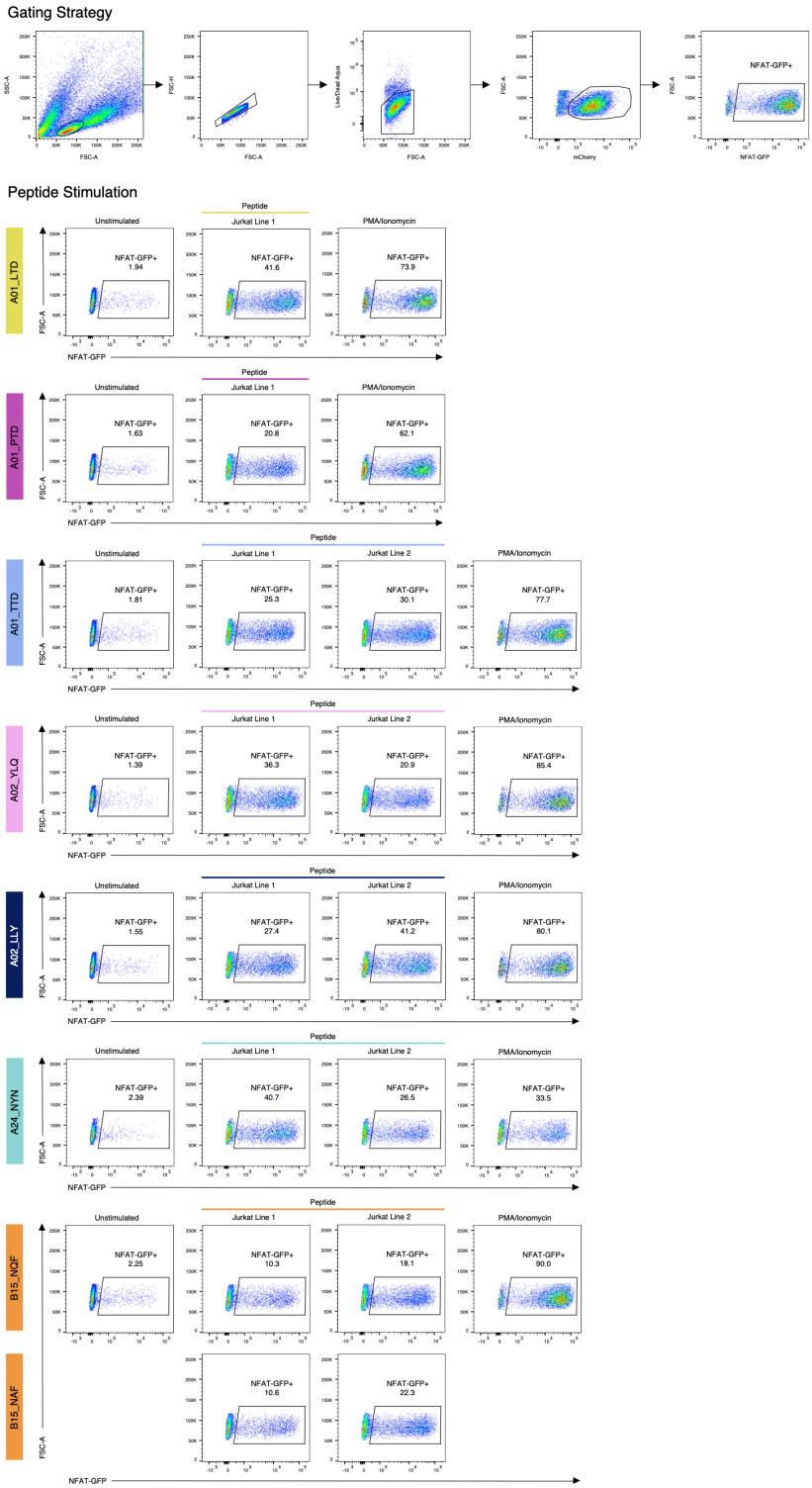

Extended data Fig. 17. Peptide stimulation confirms specificity of αβTCR motifs. Top: example of the gating strategy (B15_specific Jurkat line 1, same as Fig. S4). Left column: unstimulated control. Each row shows stimulation with a single peptide (middle columns), B15 specific TCRs were stimulated with both NQKLIAN**Q**F (SARS-CoV-2) peptide and NQKLIAN**A**F (OC43 and HKU1) peptide; Right column: PMA/Ionomycin (positive control). Responsiveness of the Jurkat cell lines was determined using an endogenous NFAT-GFP reporter.

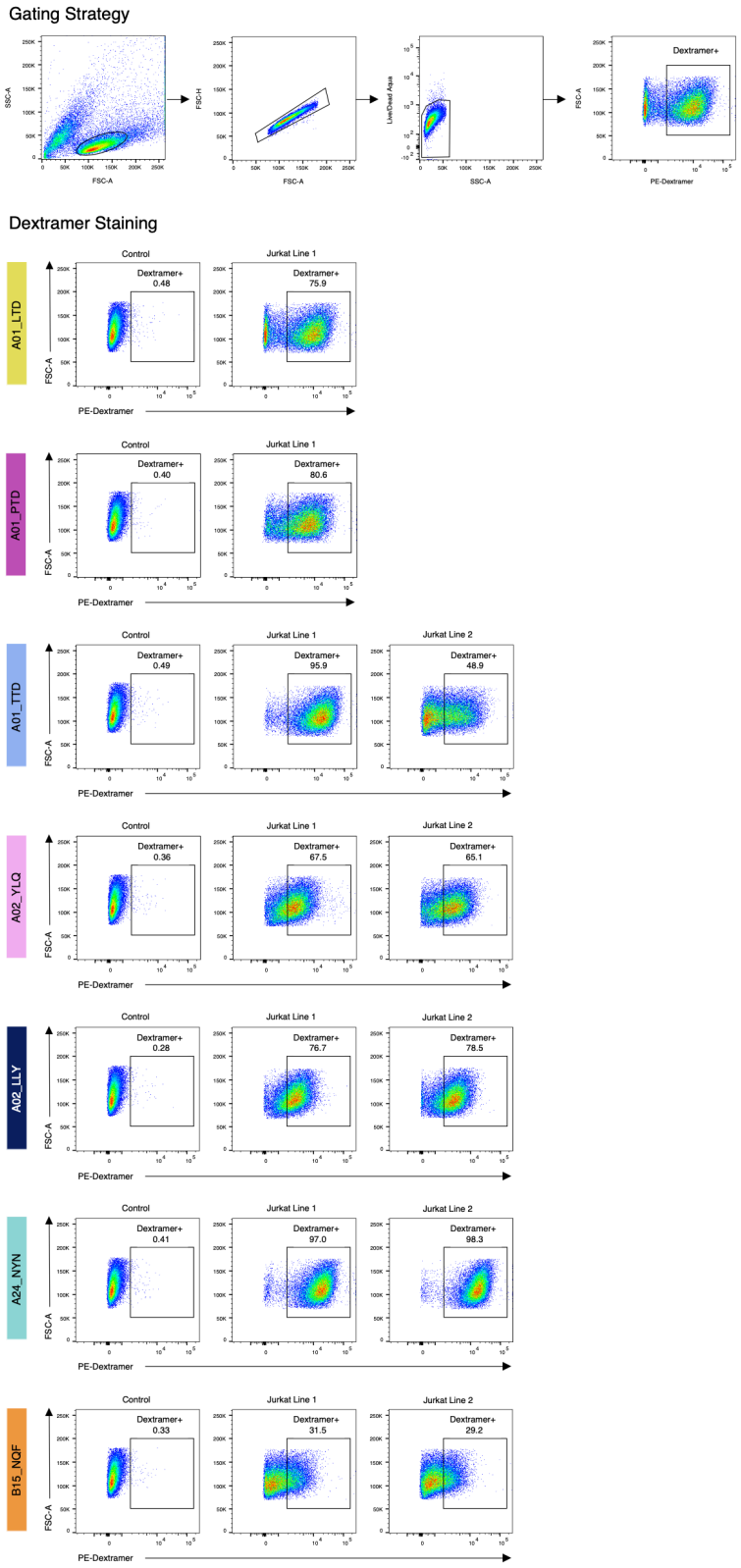

Extended data Fig. 18. MHC-dextramer staining confirms specificity of αβTCR motifs. Top: example of the gating strategy (B15_specific Jurkat line 1, same as Fig. S4). Left column: control Jurkat cell line with other known specificity. Each row shows staining with a single MHC-dextramer.

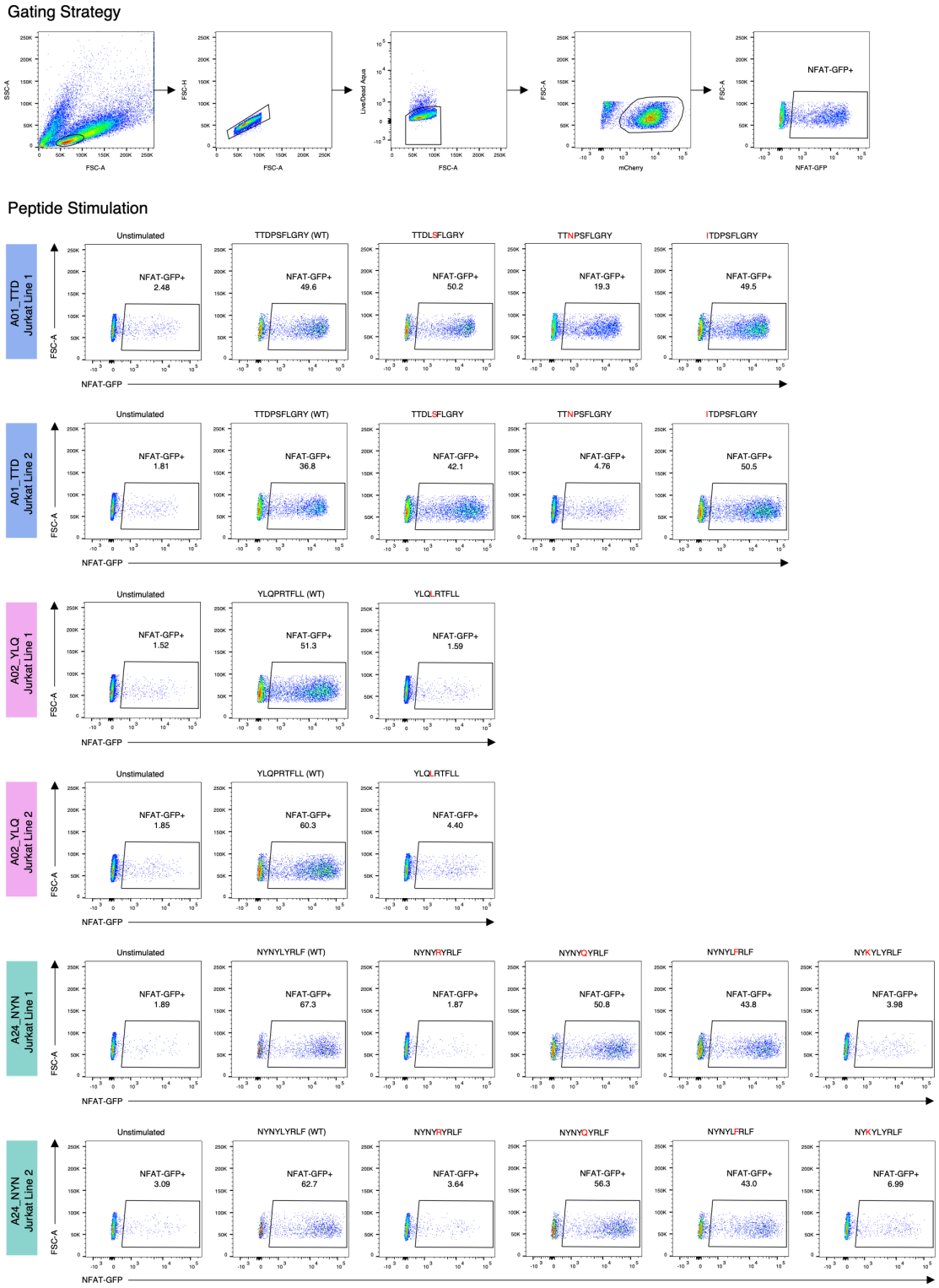

Extended data Fig. 19. Recognition of SARS-CoV-2 mutated epitopes by αβTCR motifs. Left column: unstimulated control. Each row shows stimulation with a single peptide (middle columns). Responsiveness of the Jurkat cell lines was determined using an endogenous NFAT-GFP reporter.

929 **References**

930

931 1. Flemming, A. Omicron, the great escape artist. *Nat Rev Immunol* (2022) doi:10.1038/s41577-022-
932 00676-6.

933 2. Mallajosyula, V. *et al.* CD8 $^{+}$ T cells specific for conserved coronavirus epitopes correlate with
934 milder disease in patients with COVID-19. *Sci. Immunol.* **6**, (2021).

935 3. Rydyznski Moderbacher, C. *et al.* Antigen-Specific Adaptive Immunity to SARS-CoV-2 in Acute
936 COVID-19 and Associations with Age and Disease Severity. *Cell* **183**, 996-1012.e19 (2020).

937 4. Kundu, R. *et al.* Cross-reactive memory T cells associate with protection against SARS-CoV-2
938 infection in COVID-19 contacts. *Nat Commun* **13**, 80 (2022).

939 5. Peng, Y. *et al.* An immunodominant NP105–113-B*07:02 cytotoxic T cell response controls viral
940 replication and is associated with less severe COVID-19 disease. *Nat Immunol* **23**, 50–61 (2022).

941 6. Swadling, L. *et al.* Pre-existing polymerase-specific T cells expand in abortive seronegative SARS-
942 CoV-2. *Nature* **601**, 110–117 (2022).

943 7. Bange, E. M. *et al.* CD8+ T cells contribute to survival in patients with COVID-19 and hematologic
944 cancer. *Nat Med* **27**, 1280–1289 (2021).

945 8. Soresina, A. *et al.* Two X-linked agammaglobulinemia patients develop pneumonia as COVID-19
946 manifestation but recover. *Pediatr Allergy Immunol* **31**, 565–569 (2020).

947 9. Oberhardt, V. *et al.* Rapid and stable mobilization of CD8+ T cells by SARS-CoV-2 mRNA vaccine.
948 *Nature* **597**, 268–273 (2021).

949 10. Reynolds, C. J. *et al.* Prior SARS-CoV-2 infection rescues B and T cell responses to variants after
950 first vaccine dose. *Science* **372**, 1418–1423 (2021).

951 11. Robinson, J. *et al.* IPD-IMGT/HLA Database. *Nucleic Acids Research* gkz950 (2019)
952 doi:10.1093/nar/gkz950.

953 12. Sahin, U. *et al.* BNT162b2 vaccine induces neutralizing antibodies and poly-specific T cells in
954 humans. *Nature* (2021) doi:10.1038/s41586-021-03653-6.

955 13. Ferretti, A. P. *et al.* Unbiased Screens Show CD8+ T Cells of COVID-19 Patients Recognize Shared

956 Epitopes in SARS-CoV-2 that Largely Reside outside the Spike Protein. *Immunity* **53**, 1095-1107.e3
957 (2020).
958 14. Francis, J. M. *et al.* Allelic variation in class I HLA determines CD8+ T cell repertoire shape and
959 cross-reactive memory responses to SARS-CoV-2. *Sci Immunol* eabk3070 (2021).
960 15. Gangaev, A. *et al.* Identification and characterization of a SARS-CoV-2 specific CD8+ T cell
961 response with immunodominant features. *Nat Commun* **12**, 2593 (2021).
962 16. Habel, J. R. *et al.* Suboptimal SARS-CoV-2−specific CD8 $^{+}$ T cell response associated with the
963 prominent HLA-A*02:01 phenotype. *Proc Natl Acad Sci USA* **117**, 24384–24391 (2020).
964 17. Kared, H. *et al.* SARS-CoV-2–specific CD8+ T cell responses in convalescent COVID-19
965 individuals. *Journal of Clinical Investigation* **131**, e145476 (2021).
966 18. Nguyen, T. H. O. *et al.* CD8+ T cells specific for an immunodominant SARS-CoV-2 nucleocapsid
967 epitope display high naive precursor frequency and TCR promiscuity. *Immunity* **54**, 1066-1082.e5
968 (2021).
969 19. Nielsen, S. S. *et al.* SARS-CoV-2 elicits robust adaptive immune responses regardless of disease
970 severity. *EBioMedicine* **68**, 103410 (2021).
971 20. Peng, Yanchun *et al.* Broad and strong memory CD4+ and CD8+ T cells induced by SARS-CoV-2 in
972 UK convalescent individuals following COVID-19. *Nat Immunol* **21**, 1336–1345 (2020).
973 21. Rha, M.-S. *et al.* PD-1-Expressing SARS-CoV-2-Specific CD8+ T Cells Are Not Exhausted, but
974 Functional in Patients with COVID-19. *Immunity* **54**, 44-52.e3 (2021).
975 22. Saini, S. K. *et al.* SARS-CoV-2 genome-wide T cell epitope mapping reveals immunodominance and
976 substantial CD8 $^{+}$ T cell activation in COVID-19 patients. *Sci. Immunol.* **6**, eabf7550 (2021).
977 23. Schreibing, F. *et al. Dissecting CD8+ T cell pathology of severe SARS-CoV-2 infection by single-cell*
978 *epitope mapping*. http://biorxiv.org/lookup/doi/10.1101/2021.03.03.432690 (2021)
979 doi:10.1101/2021.03.03.432690.
980 24. Schulien, I. *et al.* Characterization of pre-existing and induced SARS-CoV-2-specific CD8+ T cells.
981 *Nat Med* **27**, 78–85 (2021).

982 25. Sekine, T. *et al.* Robust T Cell Immunity in Convalescent Individuals with Asymptomatic or Mild
983 COVID-19. *Cell* **183**, 158-168.e14 (2020).
984 26. Shomuradova, A. S. *et al.* SARS-CoV-2 Epitopes Are Recognized by a Public and Diverse
985 Repertoire of Human T Cell Receptors. *Immunity* **53**, 1245-1257.e5 (2020).
986 27. Wherry, E. J. & Kurachi, M. Molecular and cellular insights into T cell exhaustion. *Nat Rev Immunol*
987 **15**, 486–499 (2015).
988 28. Ebinger, J. E. *et al.* Antibody responses to the BNT162b2 mRNA vaccine in individuals previously
989 infected with SARS-CoV-2. *Nat Med* **27**, 981–984 (2021).
990 29. Goel, R. R. *et al.* Distinct antibody and memory B cell responses in SARS-CoV-2 naïve and
991 recovered individuals following mRNA vaccination. *Sci. Immunol.* **6**, eabi6950 (2021).
992 30. Krammer, F. *et al.* Antibody Responses in Seropositive Persons after a Single Dose of SARS-CoV-2
993 mRNA Vaccine. *N Engl J Med* **384**, 1372–1374 (2021).
994 31. Lozano-Ojalvo, D. *et al.* Differential effects of the second SARS-CoV-2 mRNA vaccine dose on T
995 cell immunity in naive and COVID-19 recovered individuals. *Cell Reports* **36**, 109570 (2021).
996 32. Mazzoni, A. *et al.* First-dose mRNA vaccination is sufficient to reactivate immunological memory to
997 SARS-CoV-2 in subjects who have recovered from COVID-19. *Journal of Clinical Investigation*
998 **131**, e149150 (2021).
999 33. Wang, Z. *et al.* Naturally enhanced neutralizing breadth against SARS-CoV-2 one year after
1000 infection. *Nature* (2021) doi:10.1038/s41586-021-03696-9.
1001 34. Nelde, A. *et al.* SARS-CoV-2-derived peptides define heterologous and COVID-19-induced T cell
1002 recognition. *Nat Immunol* **22**, 74–85 (2021).
1003 35. Snyder, T. M. *et al. Magnitude and Dynamics of the T-Cell Response to SARS-CoV-2 Infection at*
1004 *Both Individual and Population Levels*. http://medrxiv.org/lookup/doi/10.1101/2020.07.31.20165647
1005 (2020) doi:10.1101/2020.07.31.20165647.
1006 36. Tarke, A. *et al.* Comprehensive analysis of T cell immunodominance and immunoprevalence of
1007 SARS-CoV-2 epitopes in COVID-19 cases. *Cell Reports Medicine* **2**, 100204 (2021).

1008 37. Braun, J. *et al.* SARS-CoV-2-reactive T cells in healthy donors and patients with COVID-19. *Nature*
1009 **587**, 270–274 (2020).
1010 38. Grifoni, A. *et al.* Targets of T Cell Responses to SARS-CoV-2 Coronavirus in Humans with COVID-
1011 19 Disease and Unexposed Individuals. *Cell* **181**, 1489-1501.e15 (2020).
1012 39. Le Bert, N. *et al.* SARS-CoV-2-specific T cell immunity in cases of COVID-19 and SARS, and
1013 uninfected controls. *Nature* **584**, 457–462 (2020).
1014 40. Mateus, J. *et al.* Selective and cross-reactive SARS-CoV-2 T cell epitopes in unexposed humans.
1015 *Science* **370**, 89–94 (2020).
1016 41. Diao, B. *et al.* Reduction and Functional Exhaustion of T Cells in Patients With Coronavirus Disease
1017 2019 (COVID-19). *Front. Immunol.* **11**, 827 (2020).
1018 42. Kusnadi, A. *et al.* Severely ill COVID-19 patients display impaired exhaustion features in SARS-
1019 CoV-2-reactive $CD8^+$ T cells. *Sci. Immunol.* **6**, eabe4782 (2021).
1020 43. Zheng, H.-Y. *et al.* Elevated exhaustion levels and reduced functional diversity of T cells in
1021 peripheral blood may predict severe progression in COVID-19 patients. *Cell Mol Immunol* **17**, 541–
1022 543 (2020).
1023 44. Dash, P. *et al.* Quantifiable predictive features define epitope-specific T cell receptor repertoires.
1024 *Nature* **547**, 89–93 (2017).
1025 45. Glanville, J. *et al.* Identifying specificity groups in the T cell receptor repertoire. *Nature* **547**, 94–98
1026 (2017).
1027 46. Thomas, N. *et al.* Tracking global changes induced in the CD4 T-cell receptor repertoire by
1028 immunization with a complex antigen using short stretches of CDR3 protein sequence.
1029 *Bioinformatics* **30**, 3181–3188 (2014).
1030 47. Reynisson, B., Alvarez, B., Paul, S., Peters, B. & Nielsen, M. NetMHCpan-4.1 and NetMHCIIpan-
1031 4.0: improved predictions of MHC antigen presentation by concurrent motif deconvolution and
1032 integration of MS MHC eluted ligand data. *Nucleic Acids Research* **48**, W449–W454 (2020).
1033 48. Dolton, G. *et al. Emergence of immune escape at dominant SARS-CoV-2 killer T-cell epitope*.

1034 http://medrxiv.org/lookup/doi/10.1101/2021.06.21.21259010 (2021)
1035 doi:10.1101/2021.06.21.21259010.
1036 49. Altmann, D. M., Boyton, R. J. & Beale, R. Immunity to SARS-CoV-2 variants of concern. *Science*
1037 **371**, 1103–1104 (2021).
1038 50. Geers, D. *et al.* SARS-CoV-2 variants of concern partially escape humoral but not T-cell responses in
1039 COVID-19 convalescent donors and vaccinees. *Sci. Immunol.* **6**, eabj1750 (2021).
1040 51. Tarke, A. *et al.* Impact of SARS-CoV-2 variants on the total CD4+ and CD8+ T cell reactivity in
1041 infected or vaccinated individuals. *Cell Rep Med* **2**, 100355 (2021).
1042 52. Minervina, A. A. *et al.* Longitudinal high-throughput TCR repertoire profiling reveals the dynamics
1043 of T-cell memory formation after mild COVID-19 infection. *eLife* **10**, e63502 (2021).
1044 53. Lineburg, K. E. *et al.* CD8+ T cells specific for an immunodominant SARS-CoV-2 nucleocapsid
1045 epitope cross-react with selective seasonal coronaviruses. *Immunity* **54**, 1055-1065.e5 (2021).
1046 54. Grifoni, A. *et al.* SARS-CoV-2 Human T cell Epitopes: adaptive immune response against COVID-
1047 19. *Cell Host & Microbe* S1931312821002389 (2021) doi:10.1016/j.chom.2021.05.010.
1048 55. Harris, P. A. *et al.* Research electronic data capture (REDCap)—A metadata-driven methodology and
1049 workflow process for providing translational research informatics support. *Journal of Biomedical*
1050 *Informatics* **42**, 377–381 (2009).
1051 56. Harris, P. A. *et al.* The REDCap consortium: Building an international community of software
1052 platform partners. *Journal of Biomedical Informatics* **95**, 103208 (2019).
1053 57. Hao, Y. *et al.* Integrated analysis of multimodal single-cell data. *Cell* **184**, 3573-3587.e29 (2021).
1054 58. Schattgen, S. A. *et al.* Integrating T cell receptor sequences and transcriptional profiles by clonotype
1055 neighbor graph analysis (CoNGA). *Nat Biotechnol* (2021) doi:10.1038/s41587-021-00989-2.
1056 59. Csardi, G. & Nepusz, T. The igraph software package for complex network research. *InterJournal*
1057 **Complex Systems**, 1695 (2006).
1058 60. Jacomy, M., Venturini, T., Heymann, S. & Bastian, M. ForceAtlas2, a Continuous Graph Layout
1059 Algorithm for Handy Network Visualization Designed for the Gephi Software. *PLoS ONE* **9**, e98679

1060 (2014).

1061 61. Amanat, F. *et al.* A serological assay to detect SARS-CoV-2 seroconversion in humans. *Nat Med* **26**,

1062 1033–1036 (2020).